QCD and Nuclear Physics

Misak Sargsian
Florida International University
11-June-03, User Meeting, Jefferson Lab

I. Status of the Nuclear Physics (*personal view*)

- Potential Models
- Meson Theories
- Strong QCD

II. From Intermediate to High Energies

- New Kinematics
- New Simplifications and Challanges

III. Nuclei as a Micro Lab for Studies in Hadronic Physics

IV. Cold-Dense Nuclear Matter

V. Probing the Strong Forces

- AGS is "closed"
- Confusion Theorem
- Hard Exclusive Nuclear Reactions

Potential Models

Nuclear Hamiltonian:

$$H = -\sum_i \frac{\nabla_i^2}{2m} + \sum_{i<j} V_{ij}^{2N} + \sum_{i<j<k} V_{i,j,k}^{3N} + \ldots$$

$$V_{ij}^{2N} = V_{ij}^{\pi} + V_{ij}^{Heavy\ Mesons}$$

(attractive scalar meson, and repulsive vector meson exchange)

(attractive two-pion exchange and repulsive core potentials)

- Nijmegen group analysis of 1955-1992 data at energies below the pion threshold of $350 MeV$.

- NN interaction models which fit the Nijmegen data are called modern. (Nijmegen I,II, Argone v_{18}, Reid 93, CD-Bonn).

- Some models have nonlocalities (Nijmegen I, CD-Bonn)

Three-Nucleon Interactions:$\sim$ choics of pion exchange models

Relativistic Corrections- Mainly Boost Corrections

Meson Exchange Models

$\boxed{\text{Strong Interaction could be described through}}$

$\boxed{\text{Scalar and Vector Meson Exchanges}}$

Pomeranchuk, Landau - 1950's

$\frac{g^2}{4\pi} \sim 1$

$$g^2(\Lambda^2) = \frac{g^2}{1 - 5(\frac{g^2}{4\pi})ln(\frac{\Lambda^2}{m^2})}$$

Infinite interaction occurs at transferred momenta $\approx 500 MeV/c$ or at internucleon distances $\sim 1 Fm$.

It seems we have a problem about which Nature is not aware ~ Y.Pomeranchuk

All formal quantum field theories with Yukawa type interactions contain the problem of the "Zero Charge" Pomeranchuk, Sudakov, Ter-Martirosyan, Phys. Rev. 1956

Still meson theories are attractive since they can provide both attraction (scalar exchange) and repulstion (vector exchange) between hadrons. From practical point of view it is possible to construct the lagrangian with proper parameterization of the coupling constants and use Feynman diagrams to calculate the scattering amplitudes in hadronic interaction.

Quark Structure of the nucleon posses new challanges/puzzles to Meson theories. Constituent quarks phenomenologically very successfull in discrabing even static properties of the nucleons. However they can not accomodate the meson excnages between nucleons.

Pure QCD seems to justify only pion exchange as a result of Spontaneously Broken Chiral Symmetry of QCD Lagrangian - Pions - Goldstone bosons.

Strong QCD

Jefferson Lab - Strong QCD * Institution

Many approaches in Strong (Nonperturbative) QCD, Lattice, Large N_c approximation, Soliton modles of nucleon, Instanton models.

For purposes of understanting the NN interaction - another approach is to understand the lower energy limit of high momentum transfer approximation, in which we have a picture of NN interaction as a result of quark-interchange forces.

For example NN interaction

$s \to \infty \quad t \to \infty \quad \frac{t}{s} = \text{fixed}$

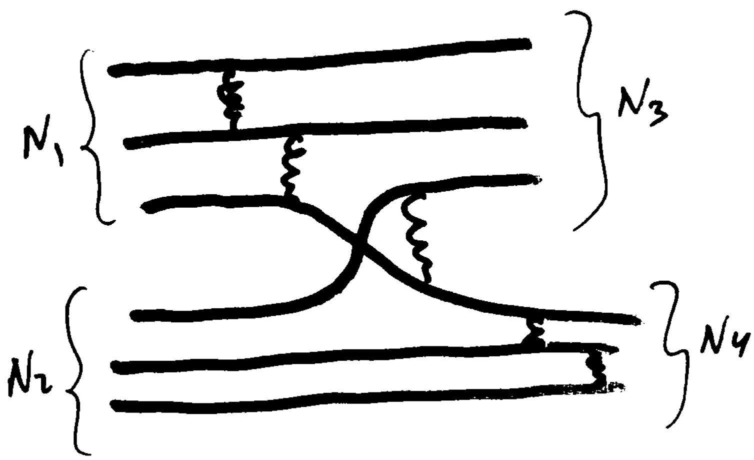

$$\frac{d\sigma}{dt} = s^{-(N_1+N_2+N_3+N_4-2)}$$

---

* *This termin I found in one of Nathan's paper, where he attributed this definition to F.Close*

II. From Intermediate to High Energies

- New Kinematics

Momenta involved in the reactions, $p \geq few\ GeV/c$.

Emergence of new small parameter

$$\frac{p_+}{p_-} \equiv \frac{E - p_z}{E + p_z} \approx \frac{m^2}{4p_z} \ll 1$$

- New Simplifications and Challanges

Consider Example of $e + d \rightarrow e' + p + n$

Some Basic Features of High Energy Small Angle Rescattering

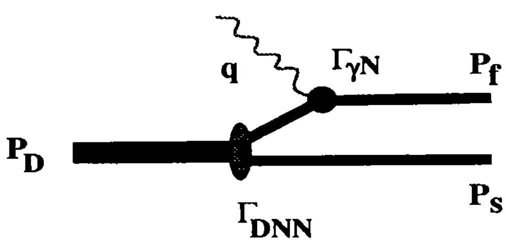

(a)

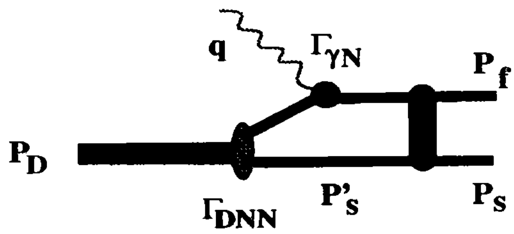

(b)

• the emergence of practically energy independent total cross section of hadron-hadron interactions at lab momenta $\geq 1 - 1.5\ GeV/c$ (total cross sections are being constant up to momenta of 400 GeV/c).

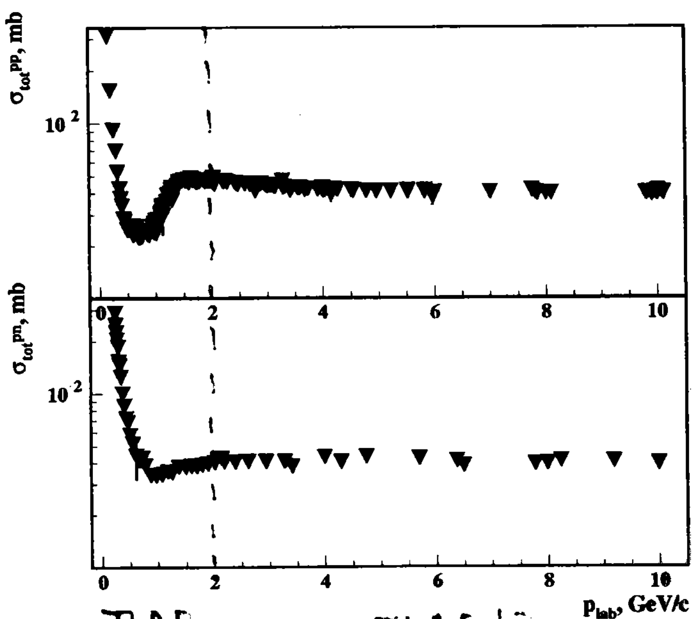

JLAB

NOW

JLAB 12

$$\left(\frac{\text{diagonal}}{\text{Charge Exchange}}\right)^{-1}$$

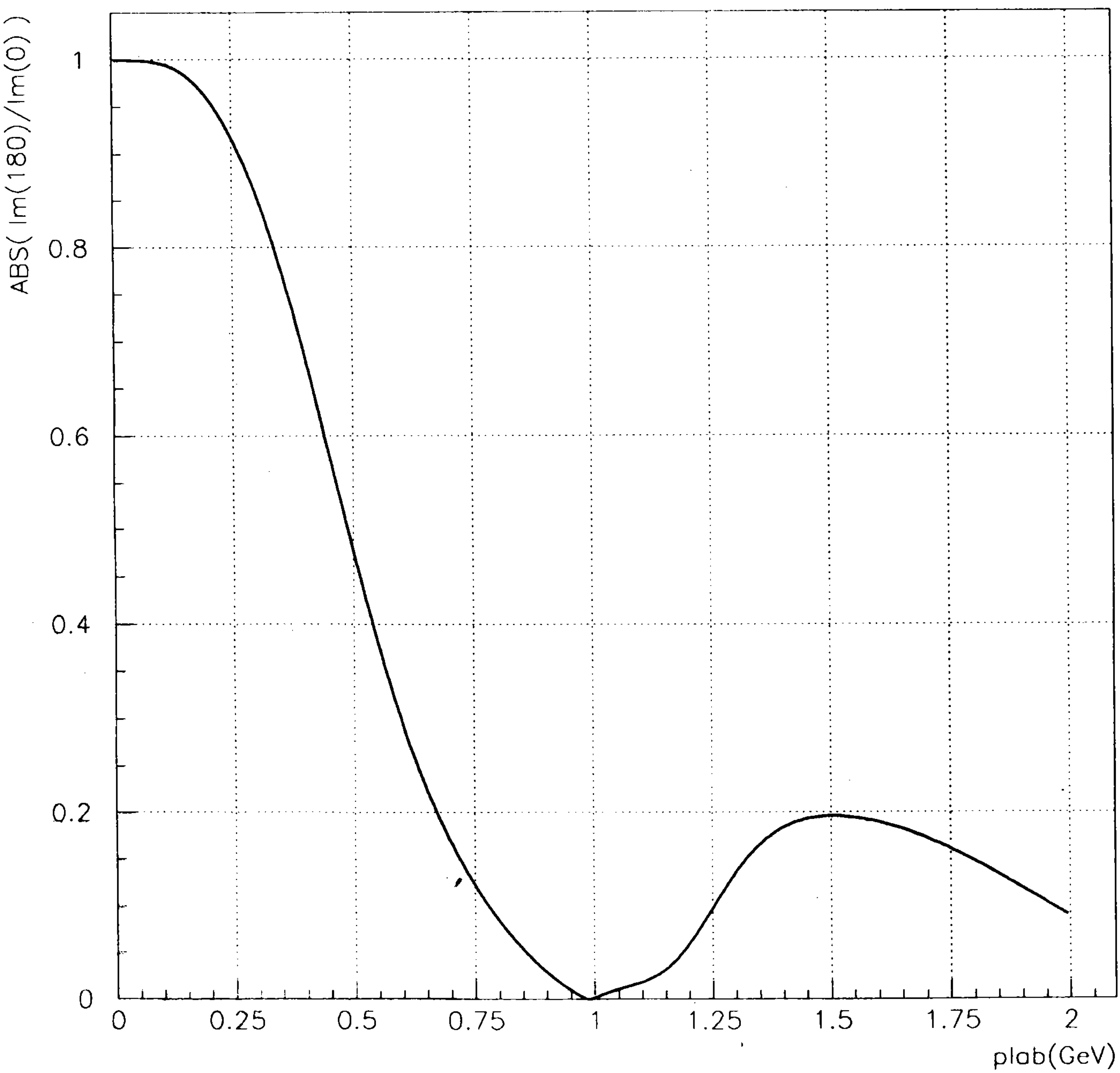

• New (Approximate) Conservation Rule

Due to FSI the reconstructed missing momenta does not coincide with the actual momenta of the bound nucleon in the nucleus (for example $\mathbf{p}'_m \neq \mathbf{p}_m = \mathbf{p}_f - \mathbf{q}$)

For this let us consider the propagation of a fast nucleon with four-momentum $k_1 = (\epsilon_1, k_{1z}, 0)$ through the nuclear medium.

We chose the z axis in the direction of $\mathbf{k}_1$ such that $\frac{k_{1-}}{m} \approx \frac{m}{2k_{1z}} \ll 1$.

After the small angle rescattering of this nucleon with the bound nucleon of four-momentum $p_1 = (E_1, p_{1z}, p_{1\perp})$, the energetic nucleon still attains its high momentum and leading z direction having now the four-momentum $k_2 = (\epsilon_2, k_{2z}, k_{2\perp})$ with $\frac{k^2_{2\perp}}{m^2_N} \ll 1$ and the bound nucleon four-momentum becomes $p_2 = (E_2, p_{2z}, p_{2\perp})$.

The energy momentum conservation for this scattering allows us to write for the "$-$" component:

$$k_{1-} + p_{1-} = k_{2-} + p_{2-}. \tag{4}$$

$$\frac{\Delta p_-}{m} \equiv \frac{p_{2-} - p_{1-}}{m} \equiv \alpha_2 - \alpha_1 = \frac{k_{1-} - k_{2-}}{m} \ll 1, \tag{5}$$

where we defined $\alpha_i = \frac{p_{i-}}{m}$, $i = 1, 2$ and used the fact that $\frac{k^2_{2\perp}}{m^2_N}, \frac{k^2_{1\perp}}{m^2_N} \ll 1$.

Therefore $\alpha_1 \approx \alpha_2$.

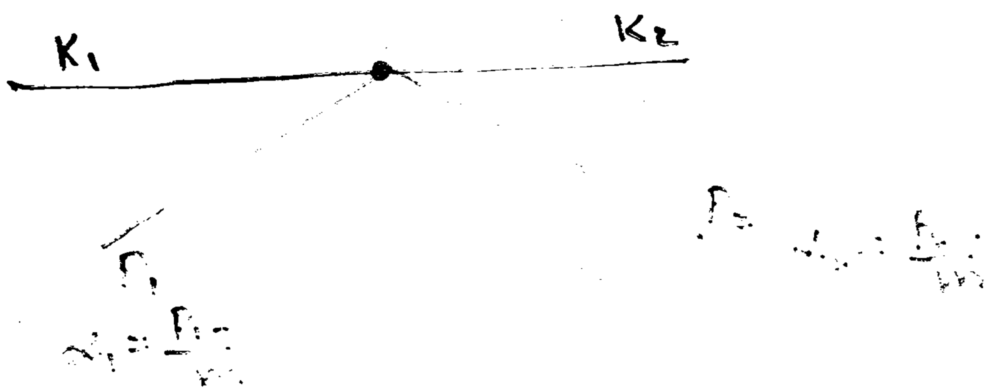

8

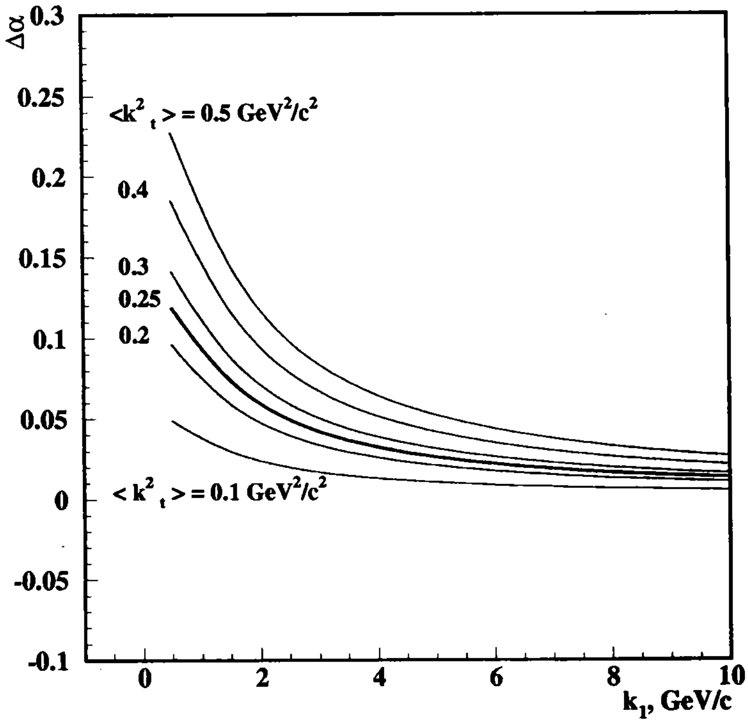
$\Delta\alpha$
0.3
0.25
0.2
0.15
0.1
0.05
0
-0.05
-0.1
$<k^2_t> = 0.5$ GeV^2/c^2
0.4
0.3
0.25
0.2
$<k^2_t> = 0.1$ GeV^2/c^2
0
2
4
6
8
10
k_l, GeV/c

9

- Reduction Theorem:

High energy particles propagating in the nuclear medium can not interact with the same bound nucleon a second time after interacting with another bound nucleon.

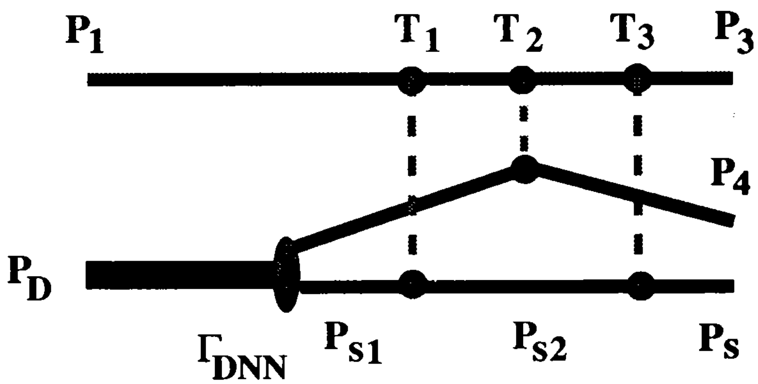

$$A_{pd\to ppn} = -\int \frac{d^4p_{s1}}{i(2\pi)^4}\frac{d^4p_{s2}}{i(2\pi)^4}\frac{T_3(p_s-p_{s2})T_2(p_4-(p_D-p_{s1}))T_1(p_{s2}-p_{s1})}{D(p_3+p_s-p_{s2})D(p_1+p_{s1}-p_{s2})} \frac{\Gamma_{DNN}}{D(p_{s2})D(p_{s1})D(p_D-p_{s1})}, \quad (6)$$

where $D(p) = -(p^2-m^2+i\epsilon)$, we neglect the spins since they are not relevant for our discussion.

$p_{1+}\sim p_{3+}\gg m$ and $p_{1-}\sim p_{3-}\ll m$
$p_{4+}\sim p_{4-}\sim p_{s+}\sim p_{s-}\sim m$

$$A_{pd\to ppn} = \frac{-1}{4}\int \frac{d^2K_\perp d^2k_{2\perp}}{(2\pi)^4}\frac{dK_-dk_{2-}}{(2\pi)^2}\frac{T_3(k_2)T_2(p_4-(p_D-p_s+K))T_1(K-k_2)}{p_{3+}(k_{2-}+i\epsilon)p_{1+}(k_{2-}-K_-+i\epsilon)} \frac{\Gamma_{DNN}}{(p_s-k_2)_-(p_s-K)_-D(p_D-p_s+K)}. \quad (7)$$

$$\int \frac{dk_{2-}dK_-}{(k_{2-}+i\epsilon)(k_{2-}-K_-+i\epsilon)} = 0. \quad (8)$$

10

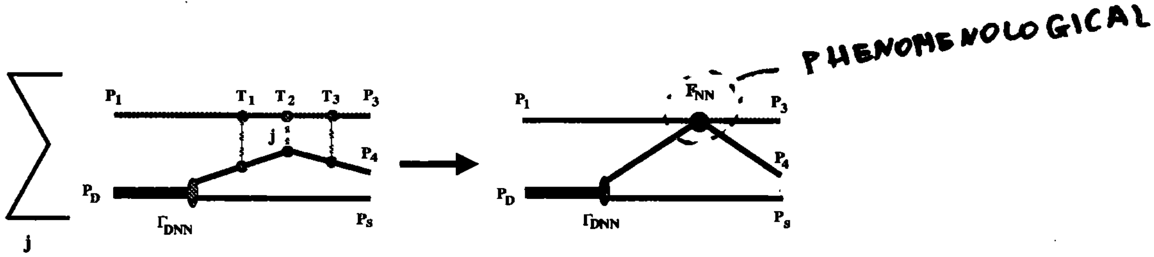

Feynman Diagram Rules for the Scattering Amplitude in GEA

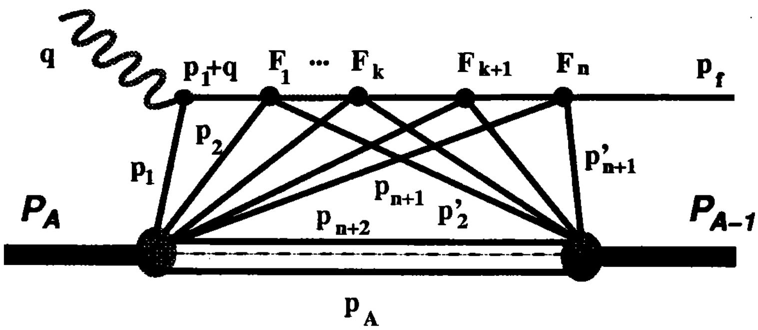

- We assigns the vertex functions $\Gamma_A(p_1,...,p_A)$ and $\Gamma^\dagger_{A-1}(p'_2,...,p_A)$ to describe the transitions between "*nucleus A*" to "*A nucleons*" with momenta $\{p_n\}$, $\{p'_n\}$ and "$(A-1)$ *nucleons*" with momenta $\{p'_n\}$ to "$(A-1)$ *nucleon final state*" respectively.
- For $\gamma^* N$ interaction we assign vertex, $F_N^{em,\mu}$.
- For each NN interaction we assign the vertex function $F_k^{NN}(p_{k+1},p'_{k+1})$. This vertex function are related to the amplitude of NN scattering as follows:

$$\bar{u}(p_3)\bar{u}(p_4)F^{NN}u(p_1)u(p_2) = \sqrt{s(s-4m^2)}f^{NN}(p_3,p_1)\delta_{\lambda,\lambda'} \approx sf^{NN}(p_3,p_1)\delta_{\lambda,\lambda'}, \tag{9}$$

where s is the total invariant energy of two interacting nucleons with momenta p_1 and p_2 and

$$f^{NN} = \sigma_{tot}^{NN}(i+\alpha)e^{-\frac{B}{2}(p_3-p_1)^2_\perp}, \tag{10}$$

where σ_{tot}^{NN}, α and B are known experimentally from NN scattering data. The vertex functions are accompanied with δ-function of energy-momentum conservation.

- For each intermediate nucleon with four momentum p we assign propagator $D(p)^{-1} = -(\hat{p} - m + i\epsilon)^{-1}$. Following to Ref.[?] we choose the "minus" sign for the nucleon propagators to simplify the calculation of the overall sign of the scattering amplitude.
- The factor $n!(A-n-1)!$ accounts for the combinatorics of n- rescatterings and $(A-n-1)$ spectator nucleons.
- For each closed contour one gets the factor $\frac{1}{i(2\pi)^4}$ with no additional sign.

Using above defined rules for the scattering amplitude of Figure 12 one obtains:

$$
\begin{aligned}
F^{(n)}_{A,A-1}(q,p_f) = & \sum_h \frac{1}{n!(A-n-1)!} \prod_{i=1}^{A}\prod_{j=2}^{A} \int d^4p_i d^4p'_j \frac{1}{\left[i(2\pi)^4\right]^{A-2+n}} \\
& \delta^4(\sum_{i=1}^{A} p_i - \mathcal{P}_A)\delta^4(\sum_{j=2}^{A} p'_j - \mathcal{P}_{A-1}) \prod_{m=n+2}^{A} \delta^4(p_m - p'_m) \times \\
& \frac{\Gamma_A(p_1,...,p_A)}{D(p_1)D(p_2)..D(p_{n+1})D(p_{n+2})..D(p_A)} \frac{F_N^{em}(Q^2)}{D(p_1+q)} \frac{f_1^{NN}(p_2,p'_2)\cdot f_n^{NN}(p_{n+2},p'_{n+2})}{D(l_1)..D(l_k)..D(l_{n-1})} \times \\
& \frac{\Gamma_{A-1}(p'_2,.p'_{n+1},.p_{n+2}..,p_A)}{D(p'_2)..D(p'_{n+1})}
\end{aligned}
\qquad (11)
$$

$$
\psi_A(p_1,p_2,...p_A) = \frac{1}{(\sqrt{(2\pi)^3 2m})^{A-1}} \frac{\Gamma_A(p_1,p_2,...p_A)}{D(p_1)}, \qquad (12)
$$

where wave functions are normalized as: $\int |\psi_A(p_1,p_2,...p_A)|^2 d^3p_1 d^2p_2..d^3p_A = 1$.

1.3 Relation of GEA to the Glauber Theory

$$\psi_D(p) = \frac{1}{(2\pi)^{\frac{3}{2}}} \int d^3r \phi_D(r) e^{-ipr}, \tag{21}$$

and using the coordinate space representation of the nucleon propagator:

$$\frac{1}{[p'_{sz} - p_{sz} + \Delta + i\epsilon]} = -i \int dz^0 \Theta(z^0) e^{i(p'_{sz} - p_{sz} + \Delta) z^0}, \tag{22}$$

we obtain the formula for the rescattering amplitude:

$$\begin{aligned} A_1^\mu &= -j^\mu(p_s + q, p_s) \frac{\sqrt{2E_s}}{2i} \int \frac{d^2k_\perp}{(2\pi)^2} d^3r \phi(r) f^{pn}(k_\perp) \theta(-z) e^{i(p_{sz} - \Delta)z} e^{i(p_{s\perp} - k_\perp)b} \\ &= -j^\mu(p_s + q, p_s) \frac{\sqrt{2E_s}}{2i} \int d^3r \phi(r) \theta(-z) \Gamma^{pn}(\Delta, -z, -b) e^{ip_s r}, \end{aligned} \tag{23}$$

where $\vec{r} = \vec{r}_p - \vec{r}_n$ and we defined a generalized profile function Γ as:

$$\Gamma^{pn}(\Delta, z, b) = \frac{1}{2i} e^{-i\Delta z} \int f^{pn}(k_\perp) e^{-ik_\perp b} \frac{d^2k_\perp}{(2\pi)^2}. \tag{24}$$

$$\Gamma^{pn}_{GA}(z,b) = \frac{1}{2i} \int f^{pn}(k_\perp) e^{-ik_\perp b} \frac{d^2k_\perp}{(2\pi)^2}$$

$$\Gamma^{pn}_{GEA}(\Delta, z, b) = e^{-i\Delta z}\, \Gamma^{pn}_{GA}(z,b)$$

1 Electro-disintegration of the Deuteron

$$Q^2 \geq 1\ GeV^2,\quad \mathbf{q} \approx \mathbf{p_f} \geq 1\ GeV/c \text{ and } |\mathbf{p_s}| \leq 400 MeV/c \tag{13}$$

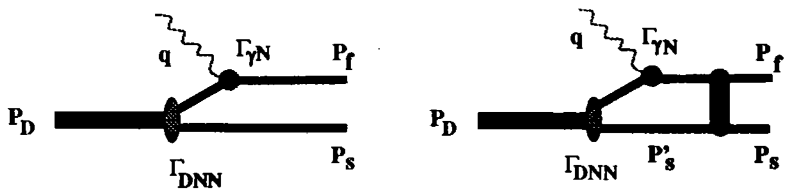

(a) (b)

VIRTUAL NUCLEON APPROXIMATION

1.1 Plane Wave Impulse Approximation

$$A_0^\mu = -\frac{\bar{u}(p_s)\bar{u}(p_f)\Gamma^\mu_{\gamma^* N}\cdot[\hat{p}_D - \hat{p}_s + m]\cdot\Gamma_{DNN}}{(p_D - p_s)^2 - m^2 + i\epsilon}. \tag{14}$$

$$A_0^\mu = \sqrt{(2\pi)^3 2E_s}\psi_D(p_s) j^\mu(p_s, q). \tag{15}$$

1.2 Single Rescattering Amplitude

To calculate the amplitude corresponding to the single rescattering - Figure 13.b, we apply the Feynman rules of Sec.VII which results:

$$A_1^\mu = -\int \frac{d^4p'_s}{i(2\pi)^4}\frac{\bar{u}(p_f)\bar{u}(p_s)F_{NN}[\hat{p}'_s + m][\hat{p}_D - \hat{p}'_s + \hat{q} + m]}{(p_D - p'_s + q)^2 - m^2 + i\epsilon}$$
$$\frac{\Gamma^\mu_{\gamma^* N}[\hat{p}_D - \hat{p}'_s + m]\Gamma_{DNN}}{((p_D - p'_s)^2 - m^2 + i\epsilon)(p'^2_s - m^2 + i\epsilon)}. \tag{16}$$

- integrate the above equation over $d^0p'_s$: $[p'^2_s - m^2 + i\epsilon]^{-1}d^0p'_s$ by $-i(2\pi)/2E'_s \approx -i(2\pi)/2m$.
- using the relation of $\hat{p}_d - \hat{p}'_s + m \approx \sum_\lambda u_\lambda(p_d - p'_s)\bar{u}_\lambda(p_d - p'_s)$ and $\hat{p}'_s + m \approx \sum_\lambda u_\lambda(p'_s)\bar{u}_\lambda(p'_s)$

$$A_1^\mu = -\frac{(2\pi)^{\frac{3}{2}}\sqrt{2E_s}}{2m} \times$$
$$\int \frac{d^3p_s'}{(2\pi)^3} \frac{sf_{pn}(p_{s\perp} - p_{s\perp}')}{(p_D - p_s' + q)^2 - m^2 + i\epsilon} \cdot j^\mu_{\gamma^* N}(p_D - p_s' + q, p_D - p_s') \cdot \psi_D(p_s').$$

- we analyze the propagator of knocked-out nucleon:

$$(p_D - p_s' + q)^2 - m^2 + i\epsilon = m_D^2 - 2p_D p_s' + p_s'^2 + 2q(p_D - p_s') - Q^2 - m^2 + i\epsilon. \quad (17)$$

the relation of energy-momentum conservation:

$$(p_D - p_s + q)^2 = m^2 = m_D^2 - 2p_D p_s + m^2 + 2q(p_D - p_s) - Q^2, \quad (18)$$

SMALL SMALL

$$(p_D - p_s' + q)^2 - m^2 + i\epsilon = 2|\mathbf{q}| \left[p_{sz}' - p_{sz} + \frac{q_0}{|\mathbf{q}|}(E_s - m) + \frac{m_D}{|\mathbf{q}|}(E_s - m) + \frac{p_s'^2 - m^2}{2|\mathbf{q}|} \right]. \quad (19)$$

- keeping only the terms which does not vanish with increase of q

$$A_1^\mu = -\frac{(2\pi)^{\frac{3}{2}}\sqrt{2E_s}}{2} \int \frac{d^3p_s'}{(2\pi)^3} \frac{f_{pn}(p_{s\perp} - p_{s\perp}')}{p_{sz}' - p_{sz} + \Delta + i\epsilon} \cdot j^\mu_{\gamma^* N}(p_D - p_s' + q, p_D - p_s') \cdot \psi_D(p_s'),$$

where

$$\boxed{\Delta = \frac{q_0}{|\mathbf{q}|}(E_s - m).} \quad (20)$$

NOT VANISHING

$$\boxed{A_1^\mu = -\frac{(2\pi)^{\frac{3}{2}}\sqrt{2E_s}}{4i} \int \frac{d^2k_t}{(2\pi)^2} f_{pn}(k_t) \cdot j^\mu_{\gamma^* N}(p_D - \tilde{p}_s + q, p_D - \tilde{p}_s) \cdot [\psi_D(\tilde{p}_s) - i\psi_D'(\tilde{p}_s)],}$$

$$k_t = p_{s\perp}' - p_{s\perp}, \; \tilde{p}_s(\tilde{p}_{sz}, \tilde{p}_{s\perp}) \equiv \tilde{\mathbf{p}}_s(p_{sz} - \Delta, p_{s\perp} - k_\perp),$$

1.4 The Cross Section of Deuteron Electro-disintegration

One can calculate now the cross section of the deuteron electro-disintegration trough the electron and deuteron electromagnetic tensors as follows:

$$\frac{d\sigma}{dE'_e d\Omega'_e d^3p_f/2E_f d^3p_s/2E_s} = \frac{E'_e}{E_e}\frac{\alpha^2}{q^4}\eta_{\mu\nu}T_D^{\mu\nu}\delta^4(p_D + q - p_f - p_s), \tag{25}$$

$$T_D^{\mu\nu} = \sum_{spin}(A_0 + A_1)^\mu (A_0 + A_1)^\nu, \tag{26}$$

FACTORIZED APPROXIMATION

$$\frac{d\sigma}{dE'_e d\Omega'_e dp_f} = p_f^2 \sigma_{eN} S_D(p_f, p_s). \tag{27}$$

The distorted spectral function can be represented as follows

$$S(p_f, p_s) = \left| \psi_D(p_s) - \frac{1}{4i}\int \frac{d^2k_t}{(2\pi)^2} f_{pn}(k_t) \cdot [\psi_D(\tilde{p}_s) - i\psi'_D(\tilde{p}_s)] \right|^2. \tag{28}$$

$$\boxed{T = \frac{\sigma^{IA+FSI}}{\sigma^{IA}} = \frac{S(p_f, p_s)}{|\psi_D(p_s)|^2}.} \tag{29}$$

SCREENING

$$T \approx 1 - \frac{1}{2}\left| \frac{\psi_D(p_s) \cdot \int \frac{d^2k_\perp}{(2\pi)^2} f_{pn}(k_\perp) \cdot [\psi_D(\tilde{p}_s) - i\psi'_D(\tilde{p}_s)]}{\psi_D^2(p_s)} \right| + \frac{1}{4}\frac{\left| \int \frac{d^2k_\perp}{(2\pi)^2} f_{pn}(k_\perp) \cdot [\psi_D(\tilde{p}_s) - i\psi'_D(\tilde{p}_s)] \right|^2}{\psi_D^2(p_s)}. \tag{30}$$

DOUBLE SCATTERING

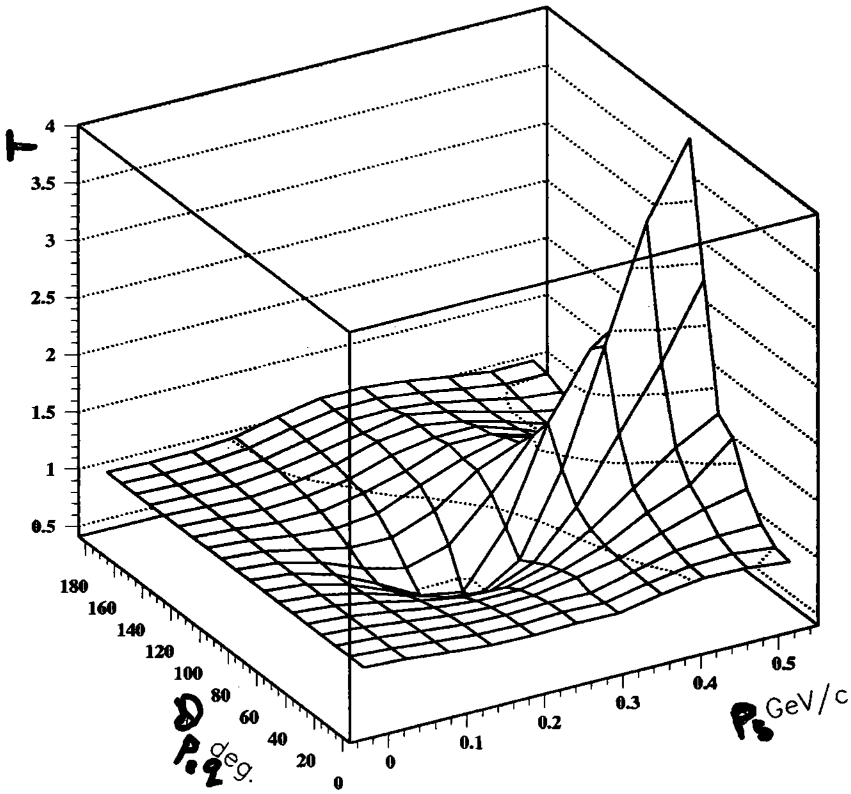

T
4
3.5
3
2.5
2
1.5
1
0.5
180
160
140
120
100
80
60
40
20
0
deg.
0
0.1
0.2
0.3
0.4
0.5
GeV/c

17

1.6 Relation to the Calculations Based on Intermediate Energy Approaches

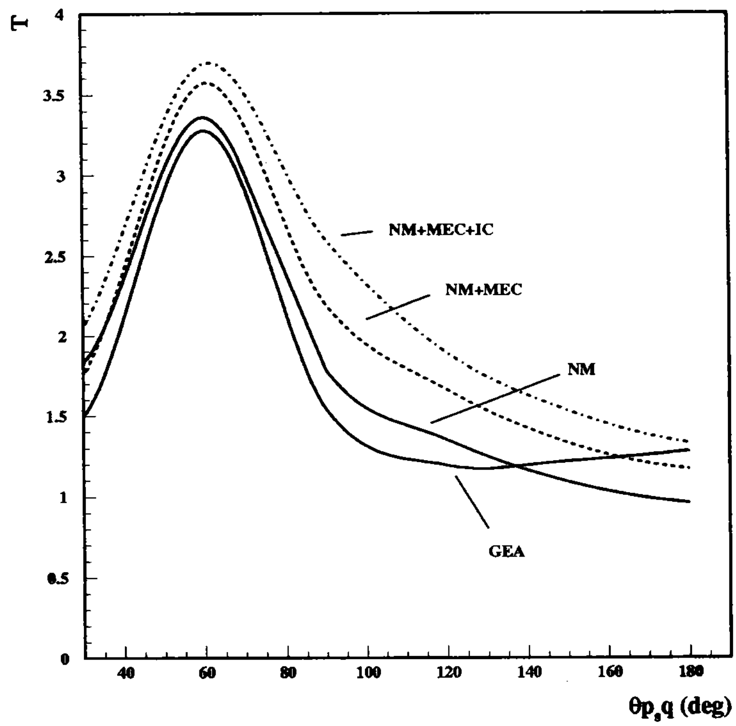

III. Nuclei as a Micro Lab for Studies in Hadronic Physics

- Using advances in understanding the wave functions of the few-nucleon systems at relatively small internal momenta

- Using the simplicities emerged due to high energy kinematics - FSI, MEC

19

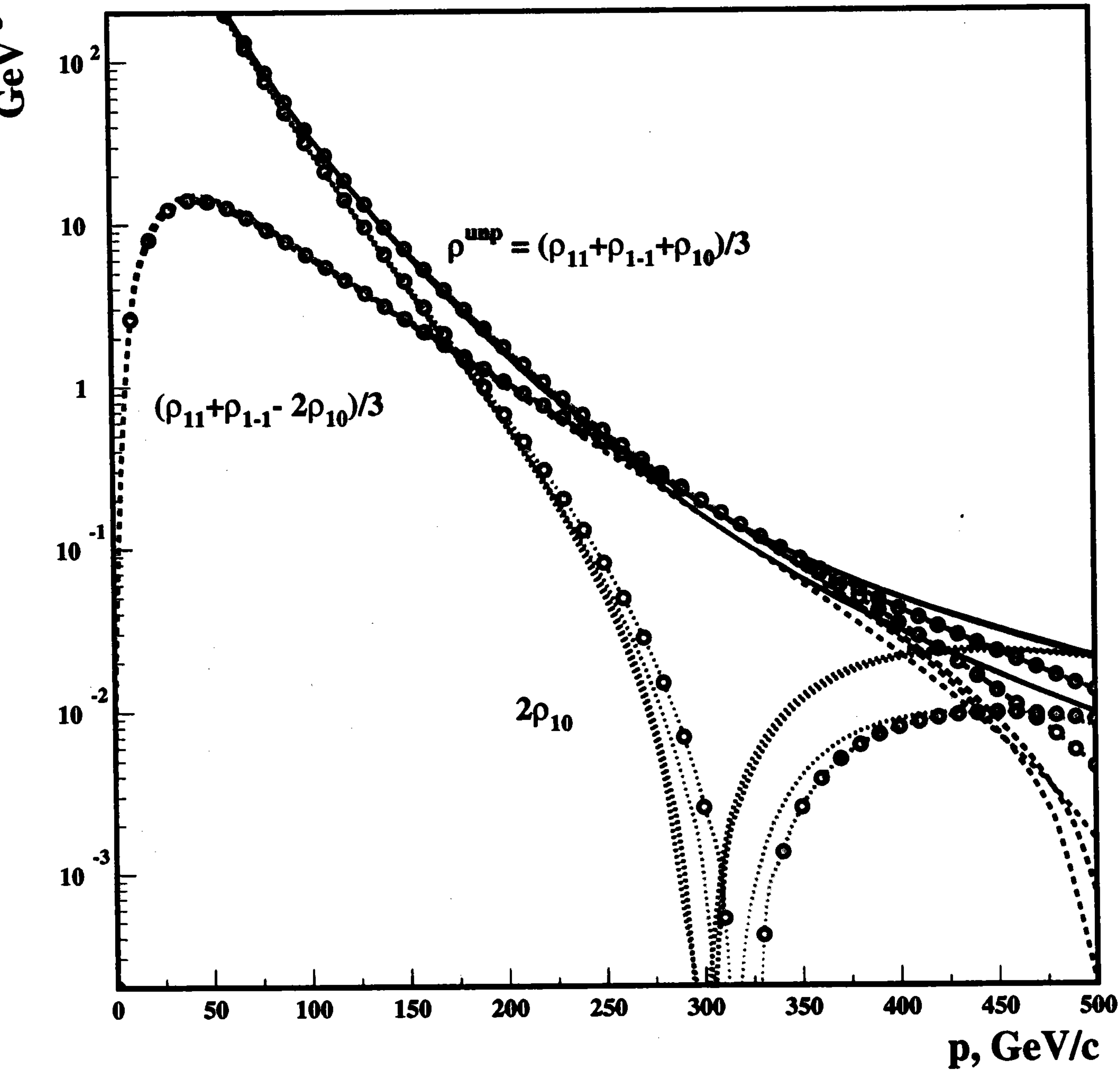
GeV
10^{2}
10
1
10^{-1}
10^{-2}
10^{-3}
0
50
100
150
200
250
300
350
400
450
500
p, GeV/c
$\rho^{unp} = (\rho_{11}+\rho_{1-1}+\rho_{10})/3$
$(\rho_{11}+\rho_{1-1}-2\rho_{10})/3$
$2\rho_{10}$

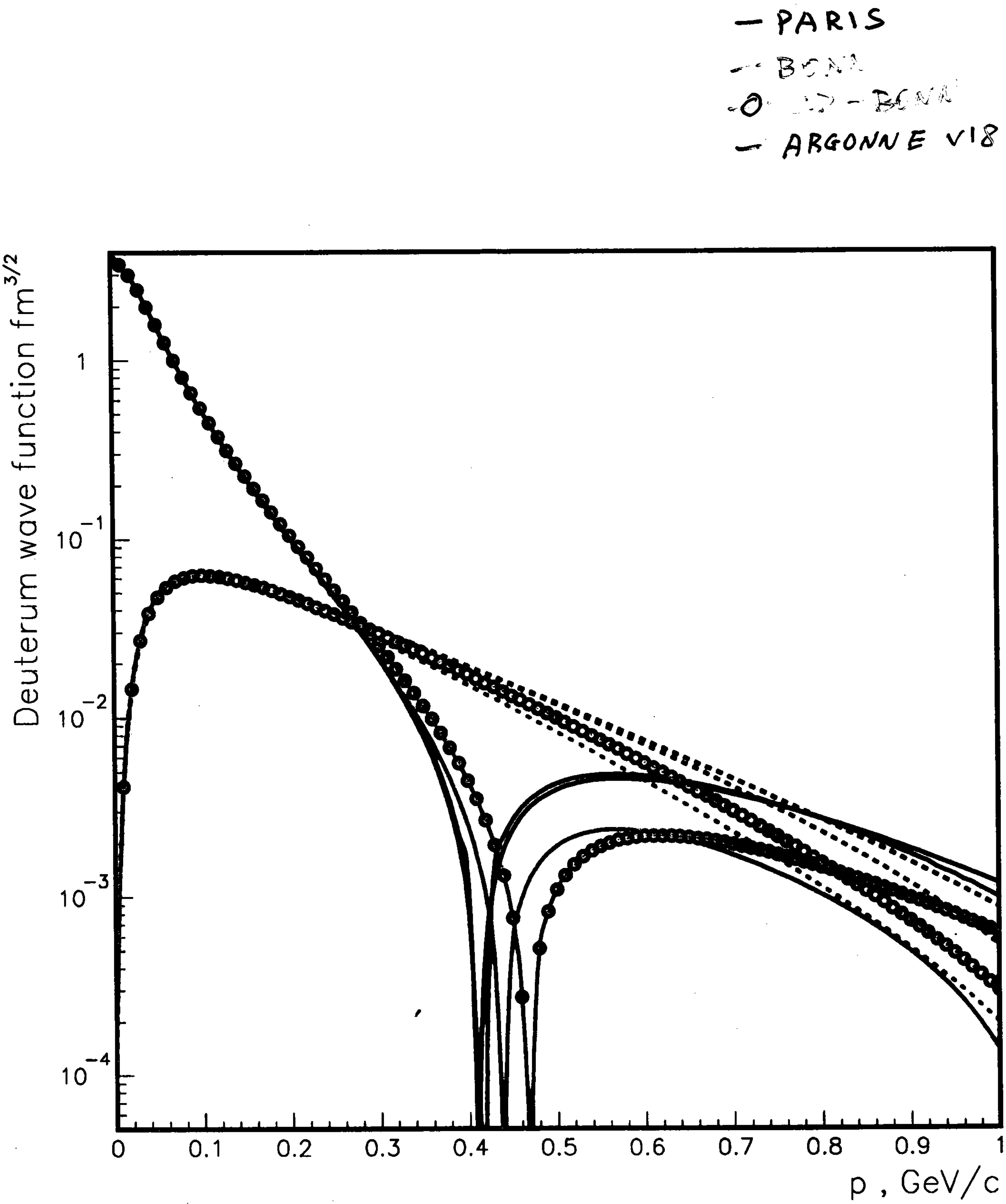
— PARIS
— ARGONNE V18
Deuterum wave function fm$^{3/2}$
1
10^{-1}
10^{-2}
10^{-3}
10^{-4}
0
0.1
0.2
0.3
0.4
0.5
0.6
0.7
0.8
0.9
1
p , GeV/c

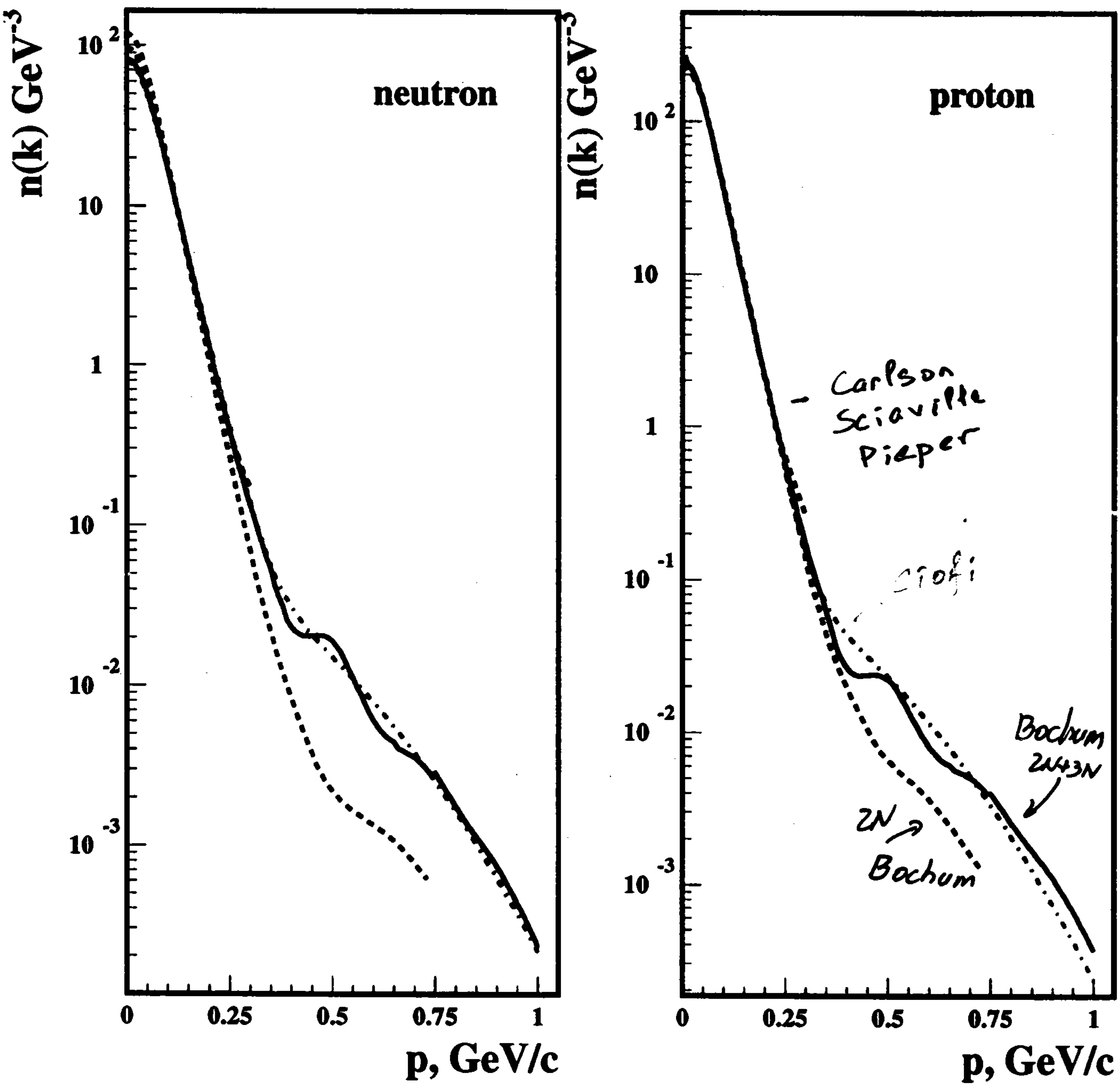
neutron
proton
n(k) GeV^-3
p, GeV/c
Carlson
Sciaville
Pieper
Ciofi
Bochum
2N+3N
2N
Bochum

$$\vec{e} + {}^3\vec{He} \rightarrow e' + n + p + p$$

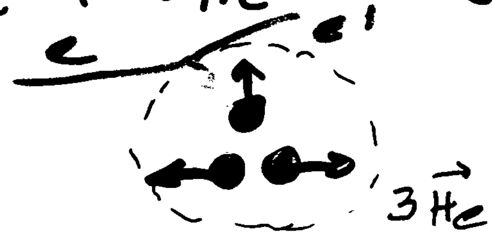

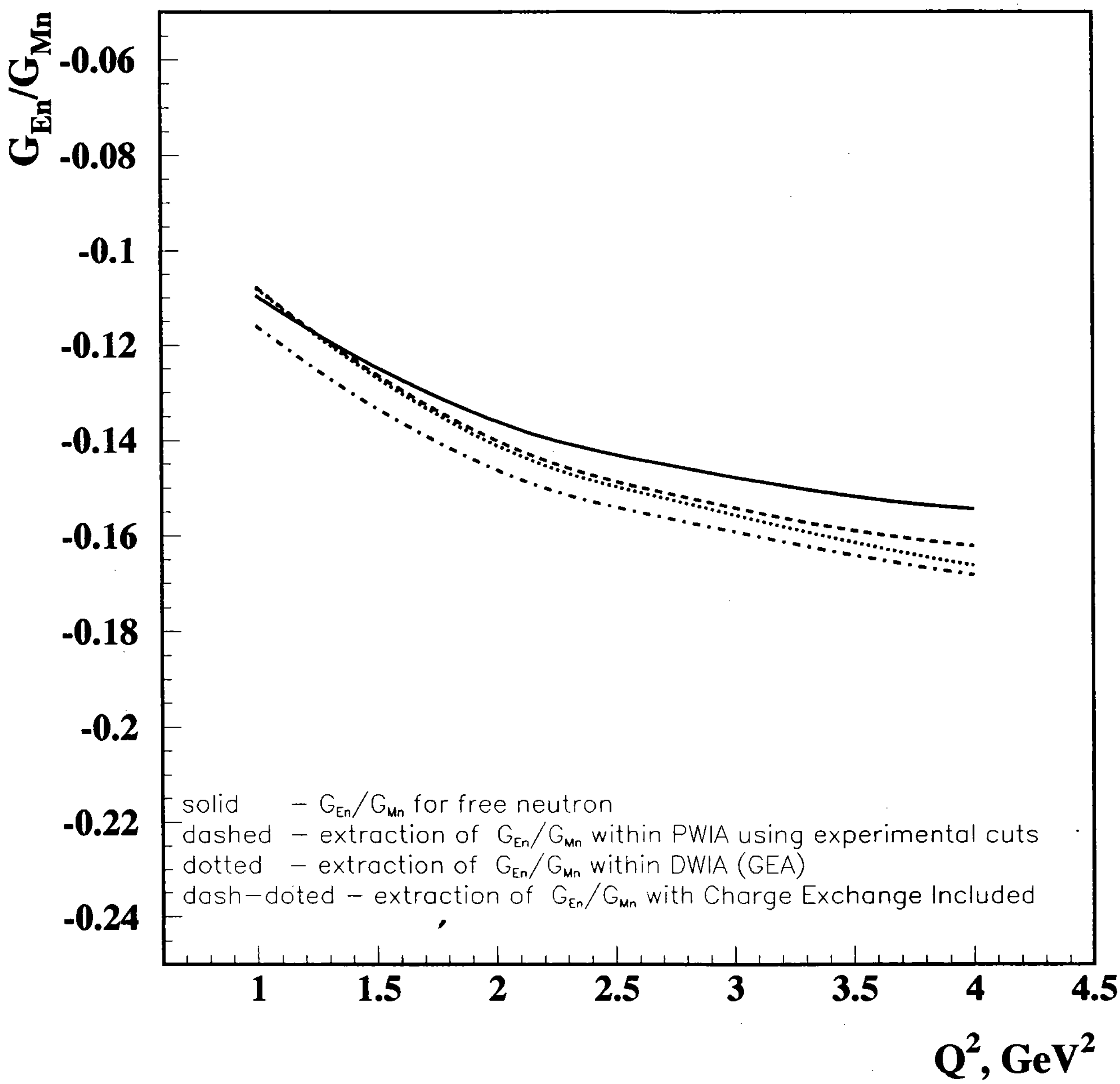

Gen Collaboration

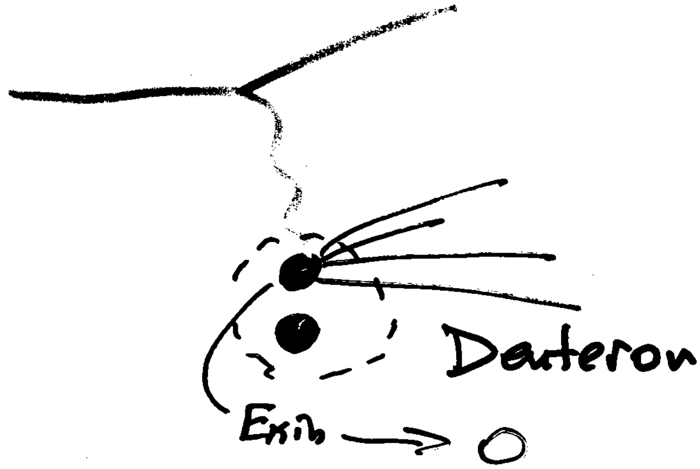

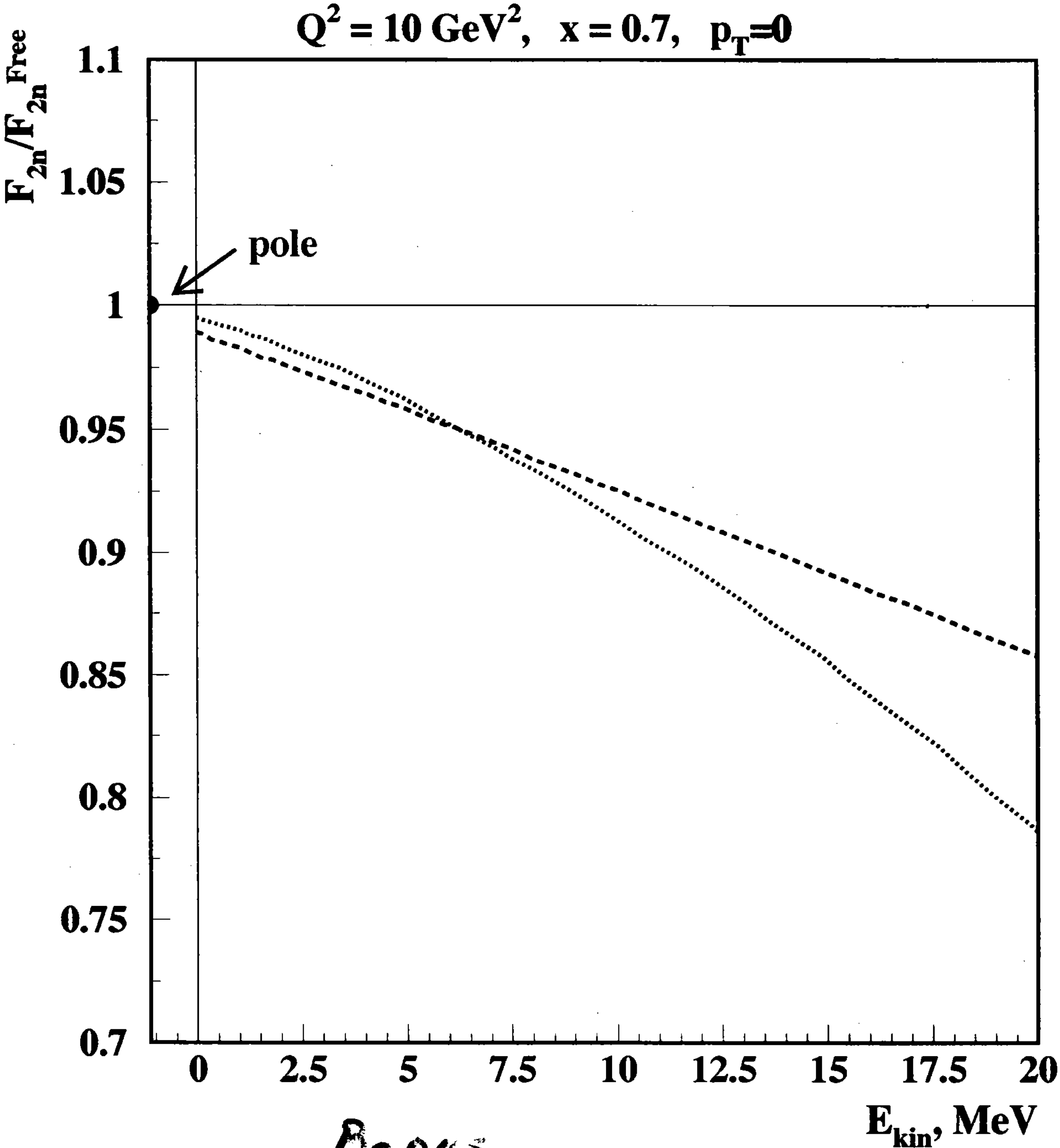

Bonus Collaboration

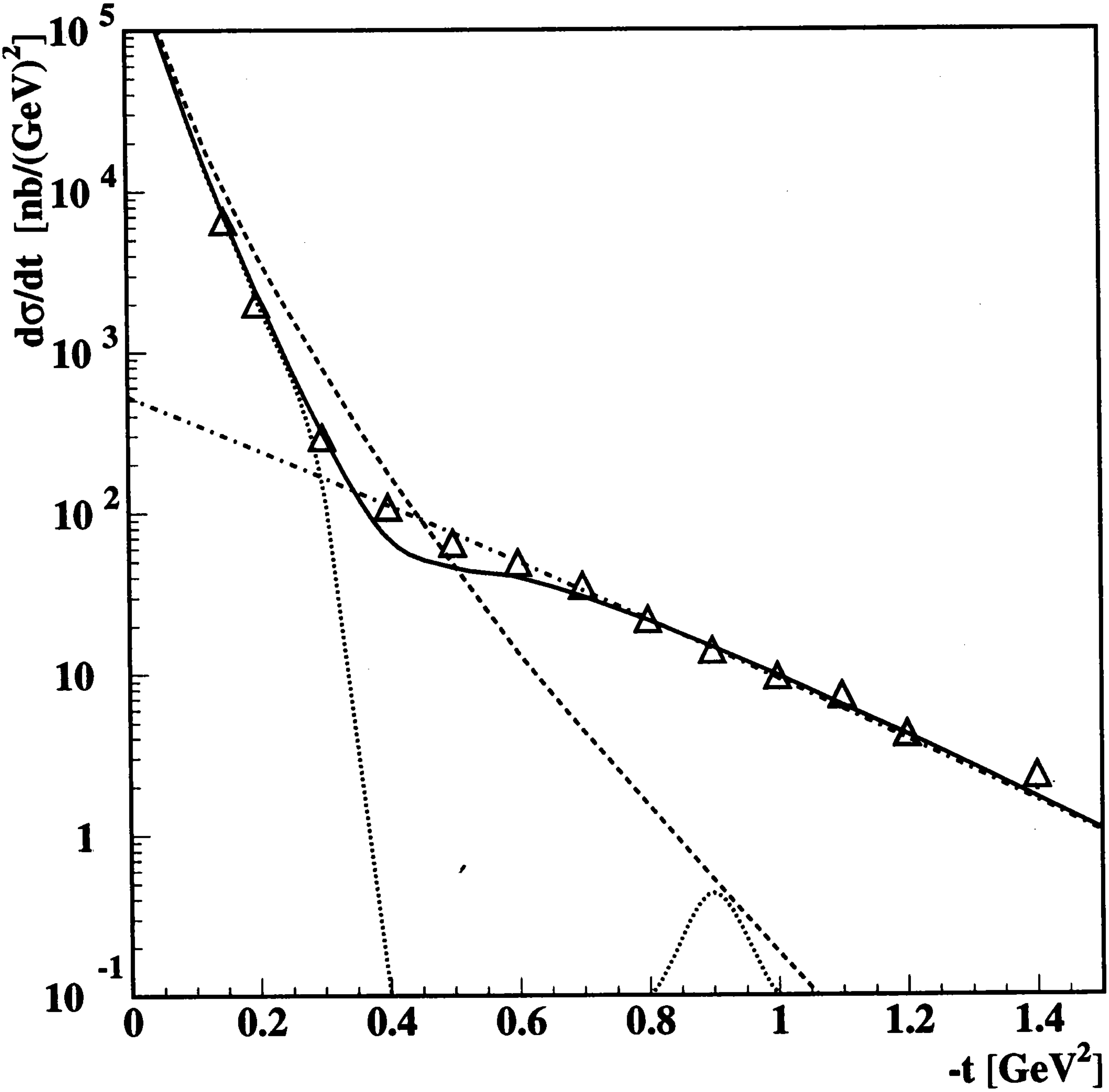

dσ/dt [nb/(GeV)^2]
10^5
10^4
10^3
10^2
10
1
10^{-1}
0
0.2
0.4
0.6
0.8
1
1.2
1.4
-t [GeV^2]

— $\sigma_{\varphi N} = 15\,mb$
- - - $\sigma_{\varphi N} = 10\,mb$

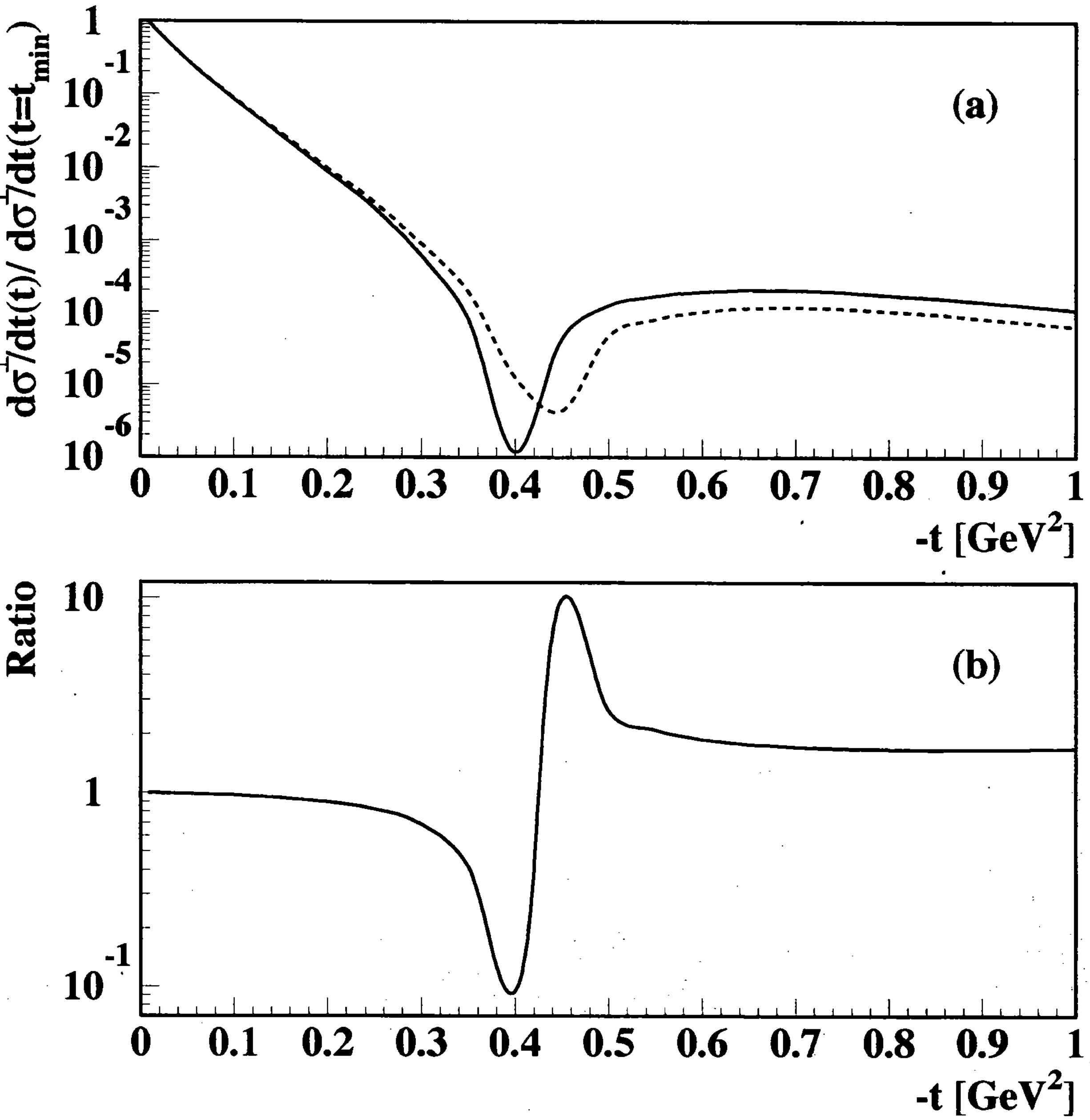

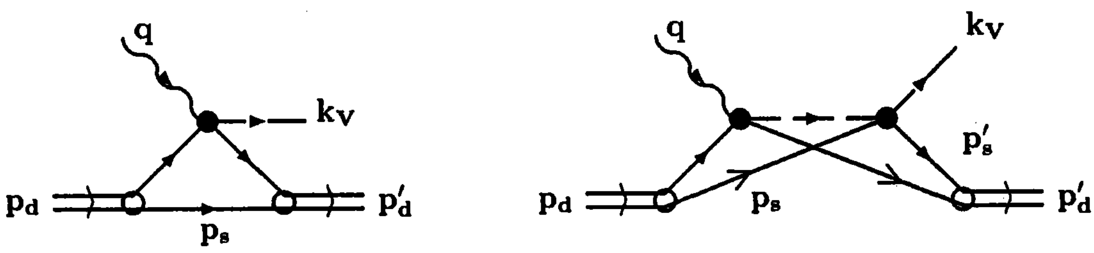

(a) (b)

Measuring σ_{VM-N} Total Cross Section

$$\gamma + d \rightarrow VM + d'$$

$$\downarrow$$

$$\rho,\ \varphi,\ J/\psi$$

IV. Cold-Dense Nuclear Matter

$\boxed{\text{Motivation}}$

- study the nuclear structure at very short space-time intervals

- nature of short-range correlations in the nuclei
- up to which limit nucleons are the relevant degrees of freedom ?
- when (if) the onset of quark-gluon degrees of freedom happen in nuclei ?
- what is the mechanism of the transition from hadronic state to quark-gluon state in nuclei ?
- if these studies probe superdense nuclear fluctuation - what is their astrophysical implications?

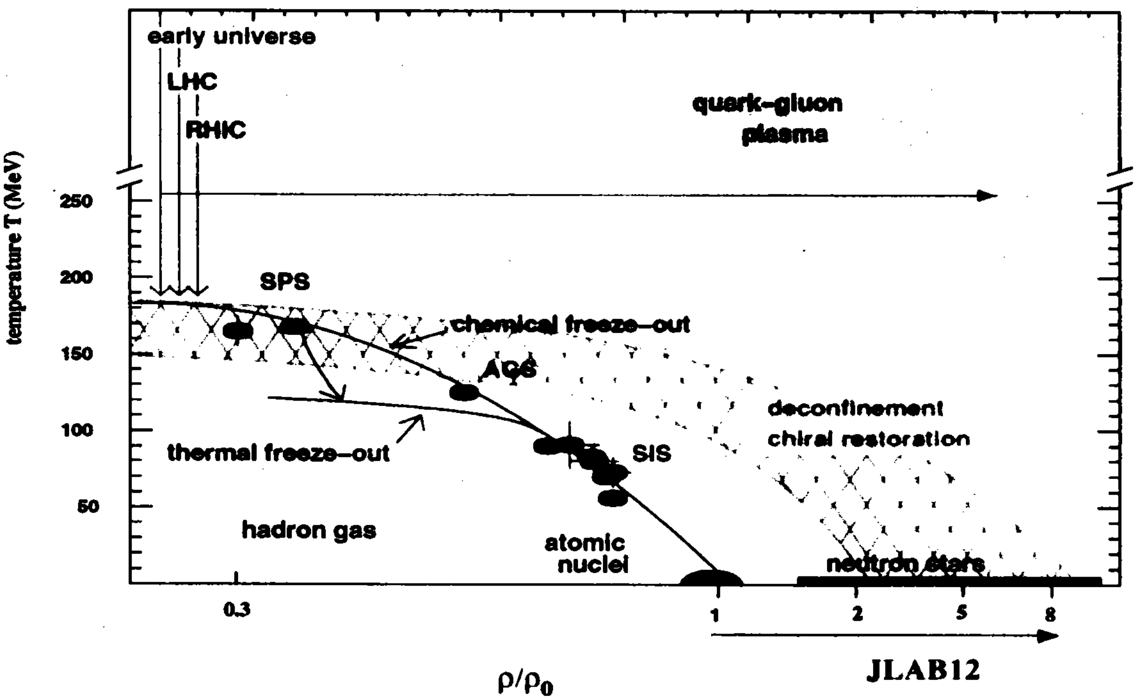

28

NN Potential

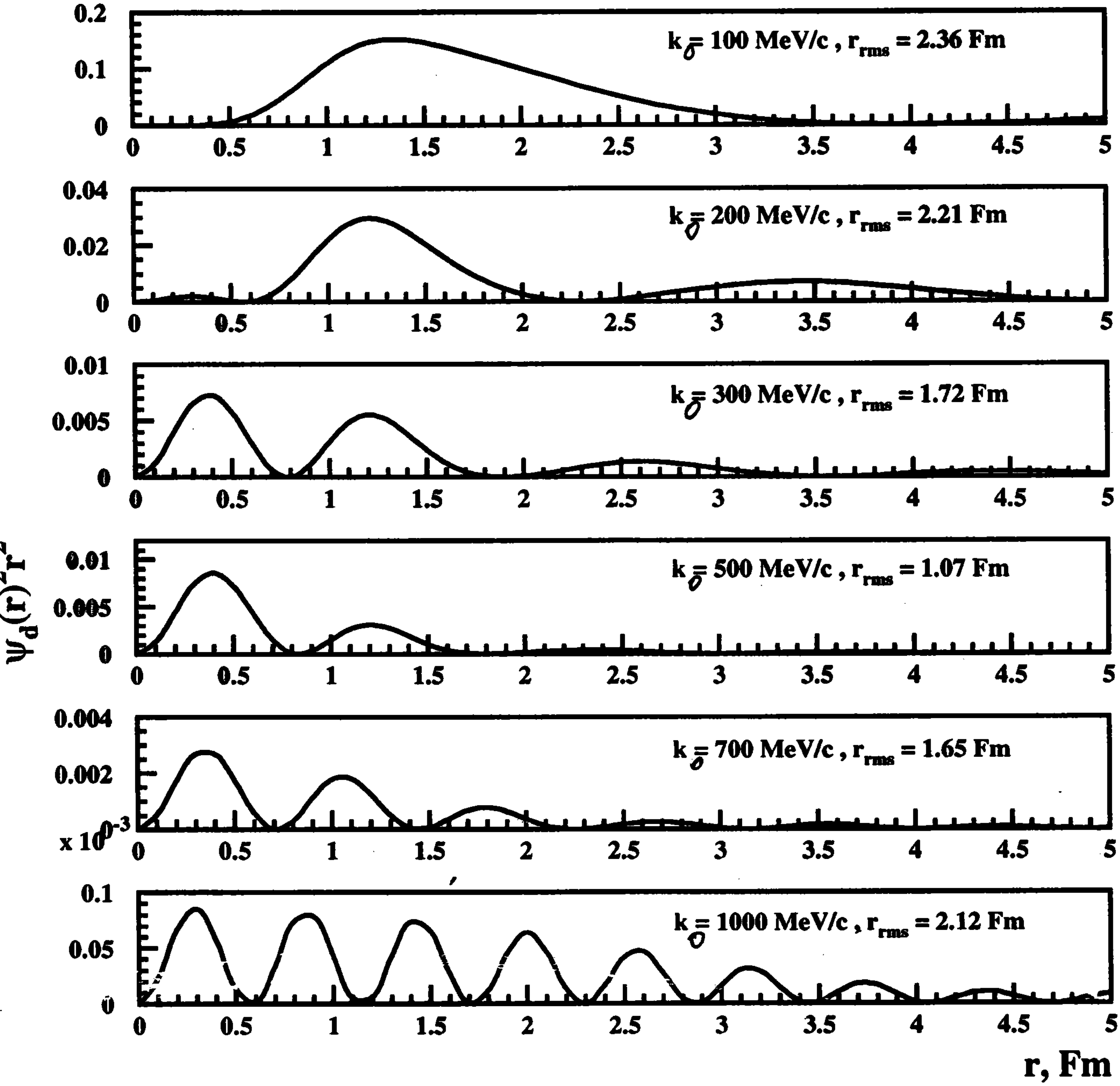

$$\Psi_D(r) = \int \theta(k-k_0)\,\frac{u(r)}{r}\,e^{-jkr}\,d^3r$$

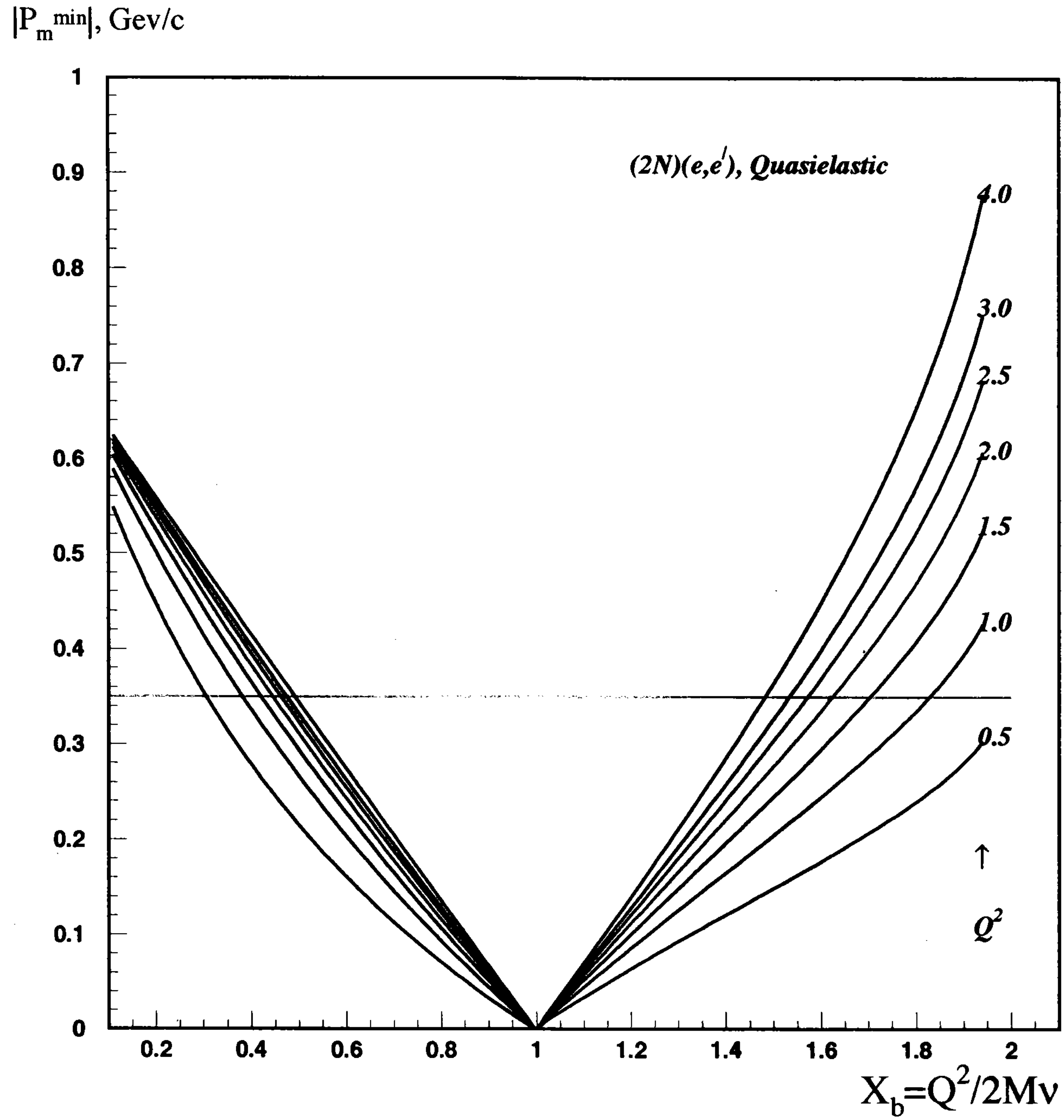

$eA \to e'(A-1)N$

$ed \to e'pn$

30

$$R_{A2}^{A1}(Q^2, x_B) = \frac{\sigma_{A_1}(Q^2, x_B)/A_1}{\sigma_{A_2}(Q^2, x_B)/A_2},$$

- **Scaling (x_B independence) is expected at $Q^2 \geq 1$ GeV^2 for $x_B^0 \leq x_B <$ 2 where x_B^0 is the threshold for high recoil momentum.**

- **No scaling is expected at $Q^2 < 1$ (GeV/c)^2.**

- **For $x_B \leq x_B^0$ the ratios should have a minimum at $x_B = 1$ and should grow with x_B since heavy nuclei have broader momentum distribution than light nuclei for $p < 0.3$ GeV/c.**

- **The onset of scaling depends on Q^2. x_B^0 should decrease with increasing Q^2.**

- **In the scaling regime, the ratios should be independent of Q^2.**

- **In the scaling regime the ratios should depend only weakly on A for $A \geq 10$. This reflects nuclear saturation.**

- **Ratios in the scaling regime are proportional to the relative probability of two-nucleon SRC in the two nuclei.**

$A(e,e')$

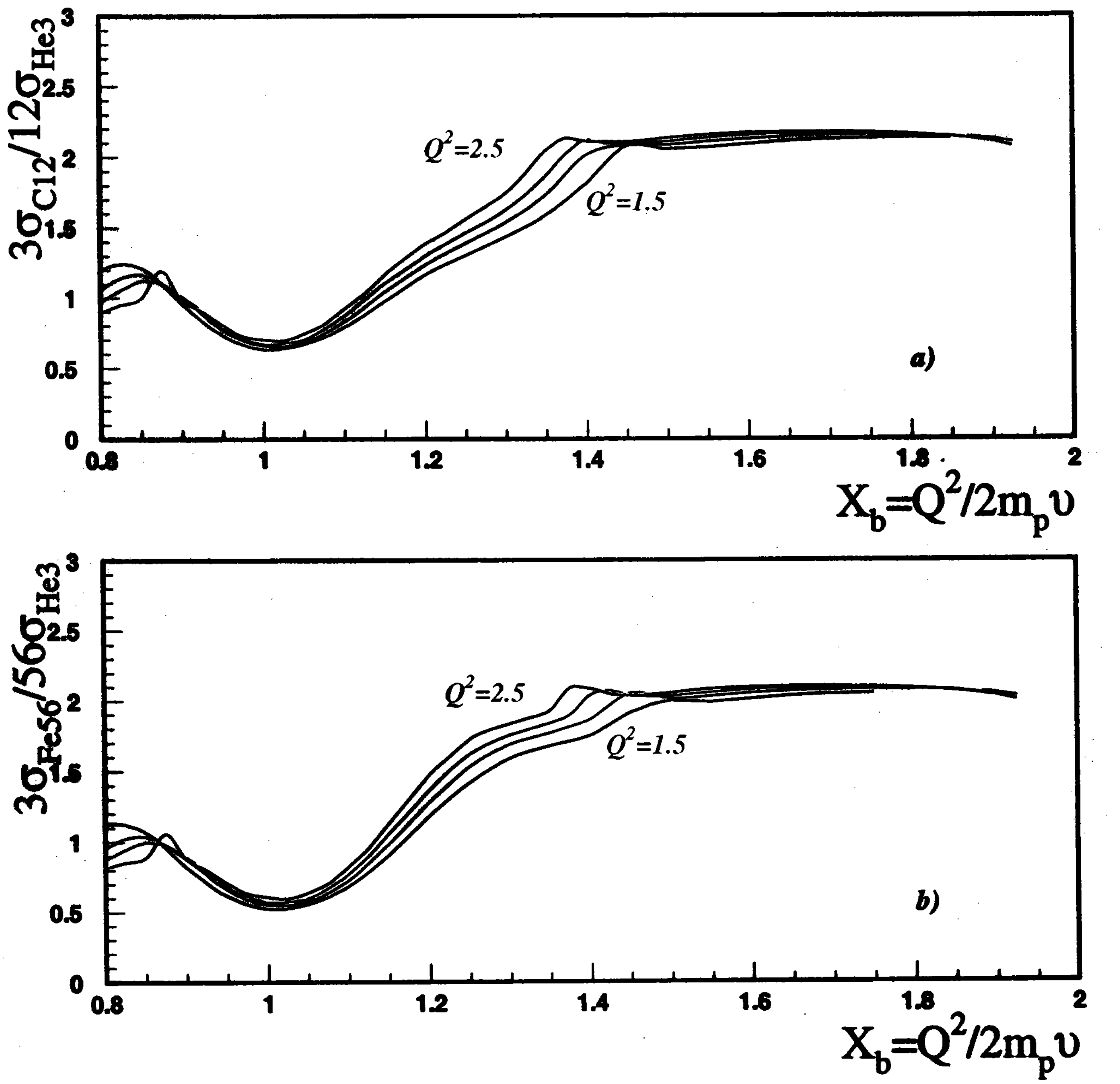

$3\sigma_{C12}/12\sigma_{He3}$
0
0.5
1
1.5
2
2.5
3
$Q^2=2.5$
$Q^2=1.5$
a)
0.8
1
1.2
1.4
1.6
1.8
2
$X_b=Q^2/2m_p\upsilon$
$3\sigma_{Fe56}/56\sigma_{He3}$
0
0.5
1
1.5
2
2.5
3
$Q^2=2.5$
$Q^2=1.5$
b)
0.8
1
1.2
1.4
1.6
1.8
2
$X_b=Q^2/2m_p\upsilon$

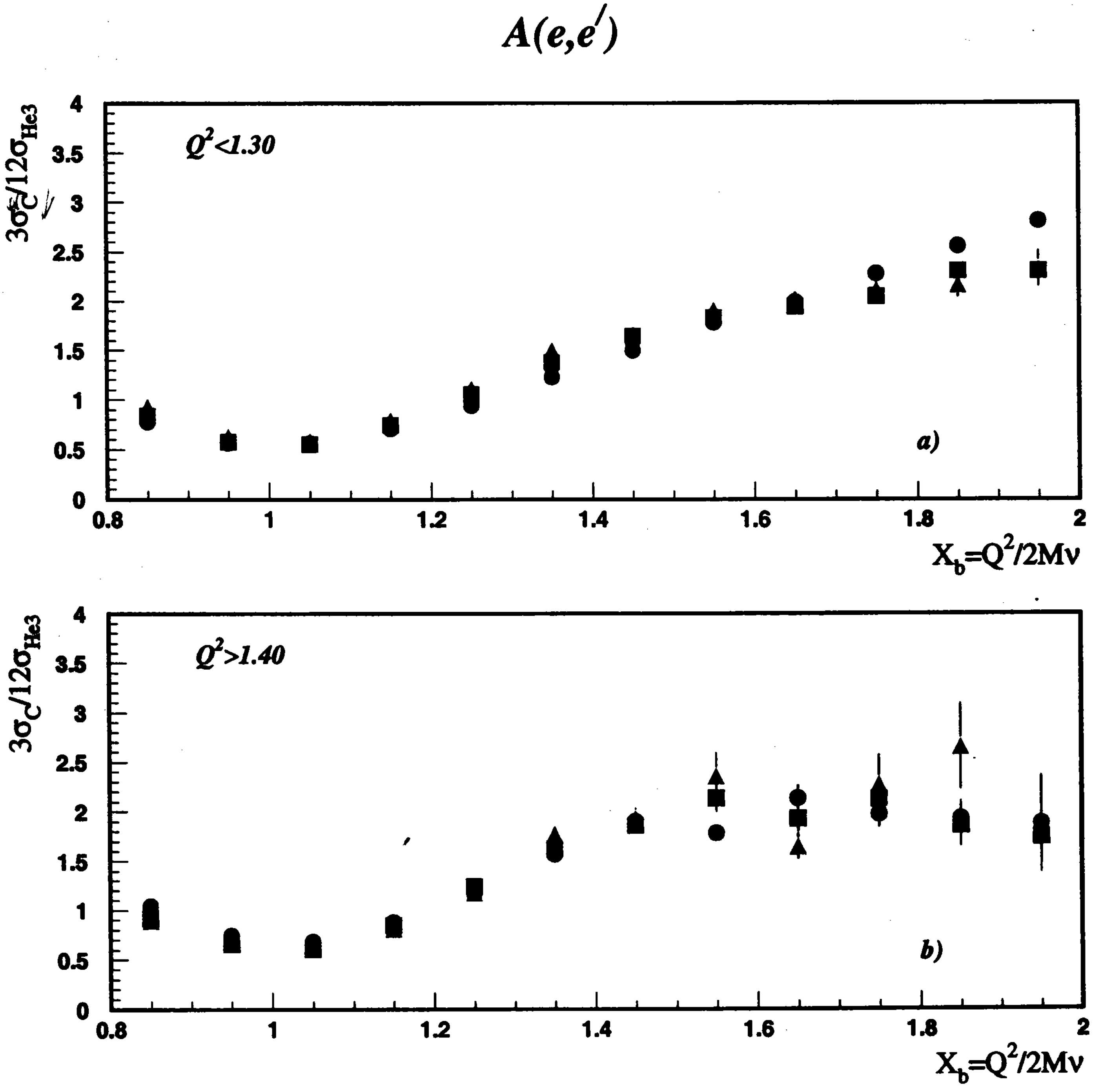
A(e,e')
$3\sigma_C/12\sigma_{He3}$
Q^2<1.30
a)
$X_b=Q^2/2M\nu$
$3\sigma_C/12\sigma_{He3}$
Q^2>1.40
b)
$X_b=Q^2/2M\nu$

33

$A(e,e')$

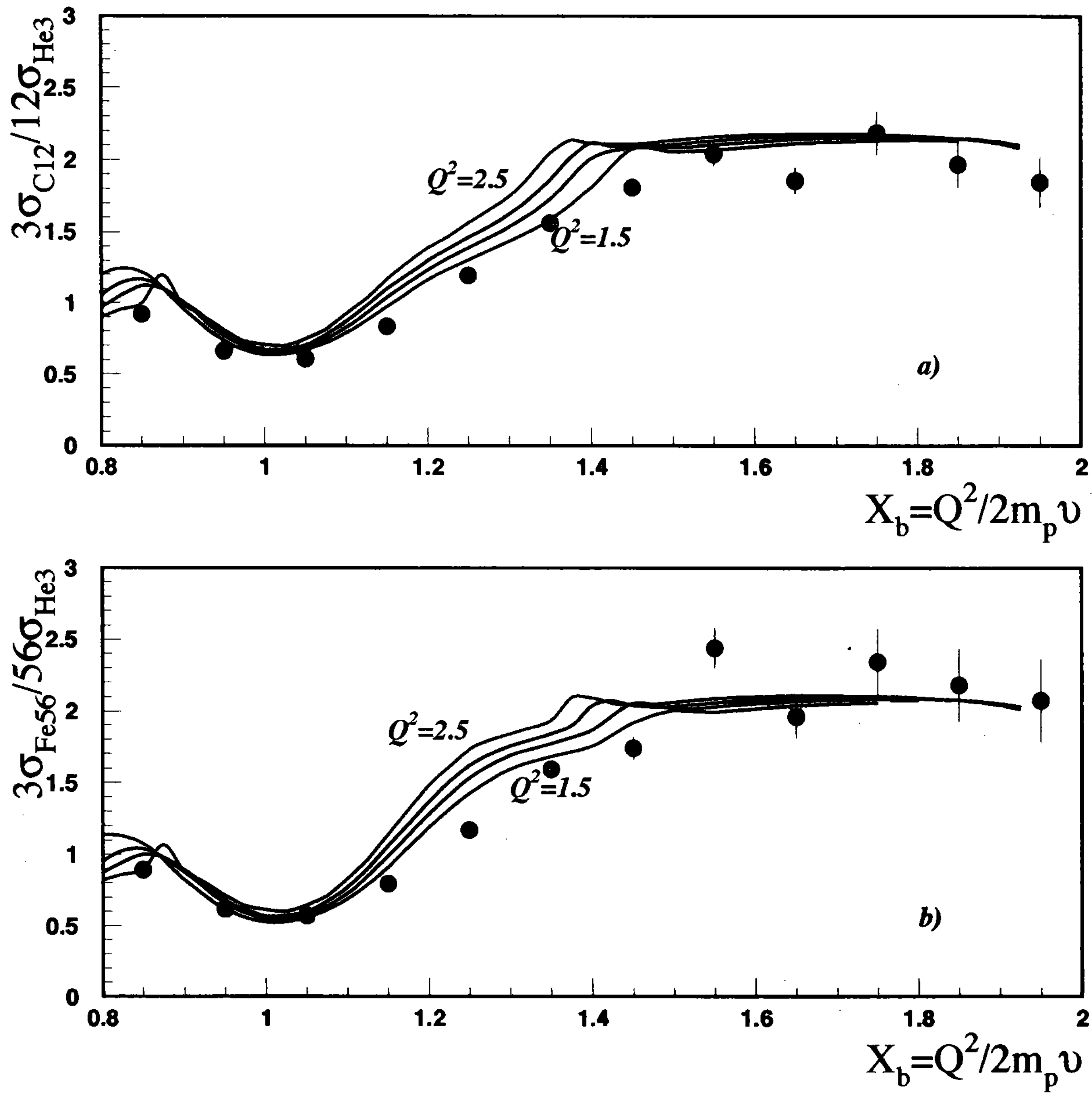

$3\sigma_{C12}/12\sigma_{He3}$
Q^2=2.5
Q^2=1.5
a)
$X_b=Q^2/2m_p\upsilon$
$3\sigma_{Fe56}/56\sigma_{He3}$
Q^2=2.5
Q^2=1.5
b)
$X_b=Q^2/2m_p\upsilon$

34

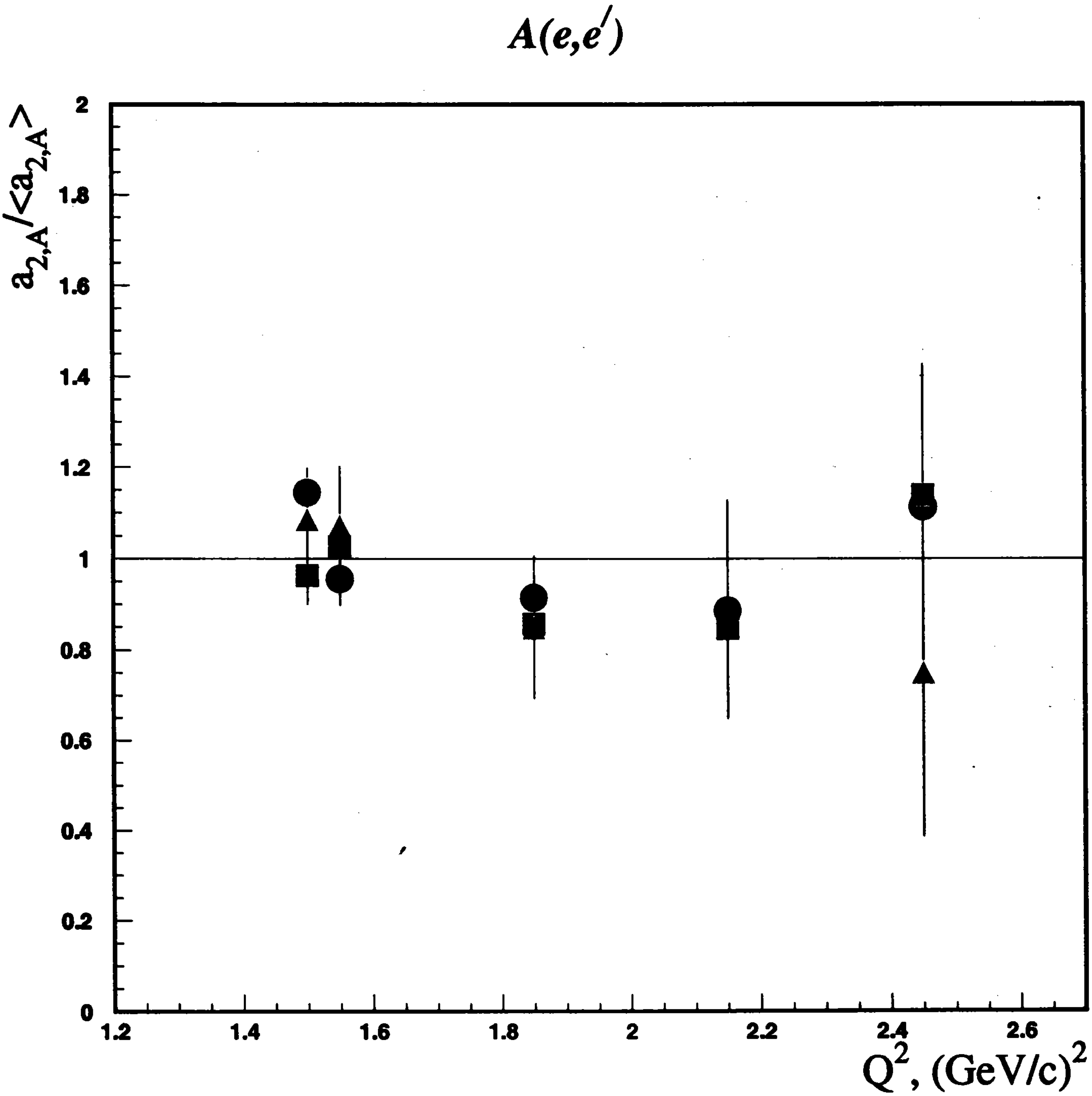
A(e,e′)
$a_{2,A}/\langle a_{2,A}\rangle$
2
1.8
1.6
1.4
1.2
1
0.8
0.6
0.4
0.2
0
1.2
1.4
1.6
1.8
2
2.2
2.4
2.6
Q^2, $(GeV/c)^2$

35

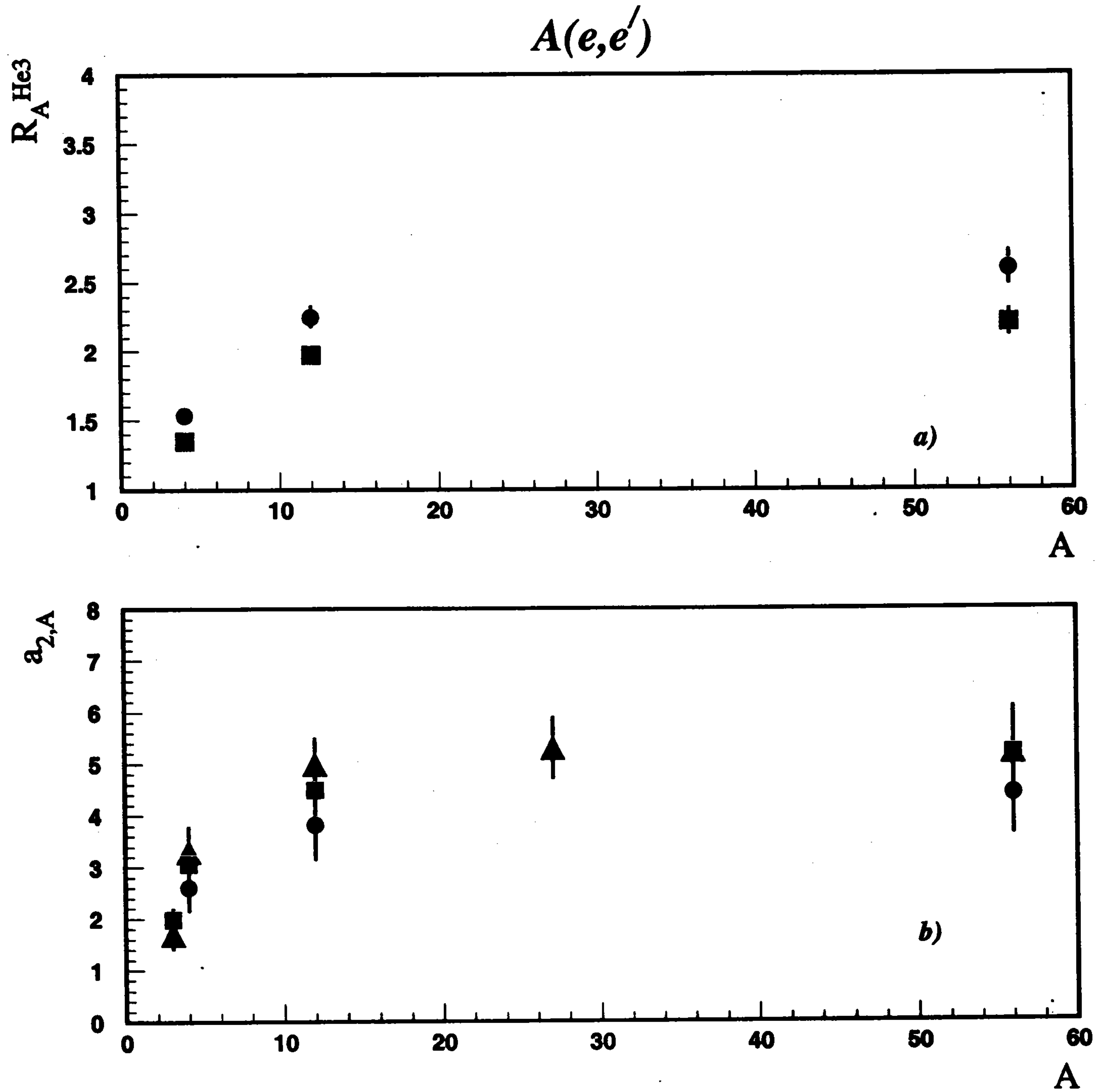

36

QUARK NUMBERS ARE NOT CONSERVED

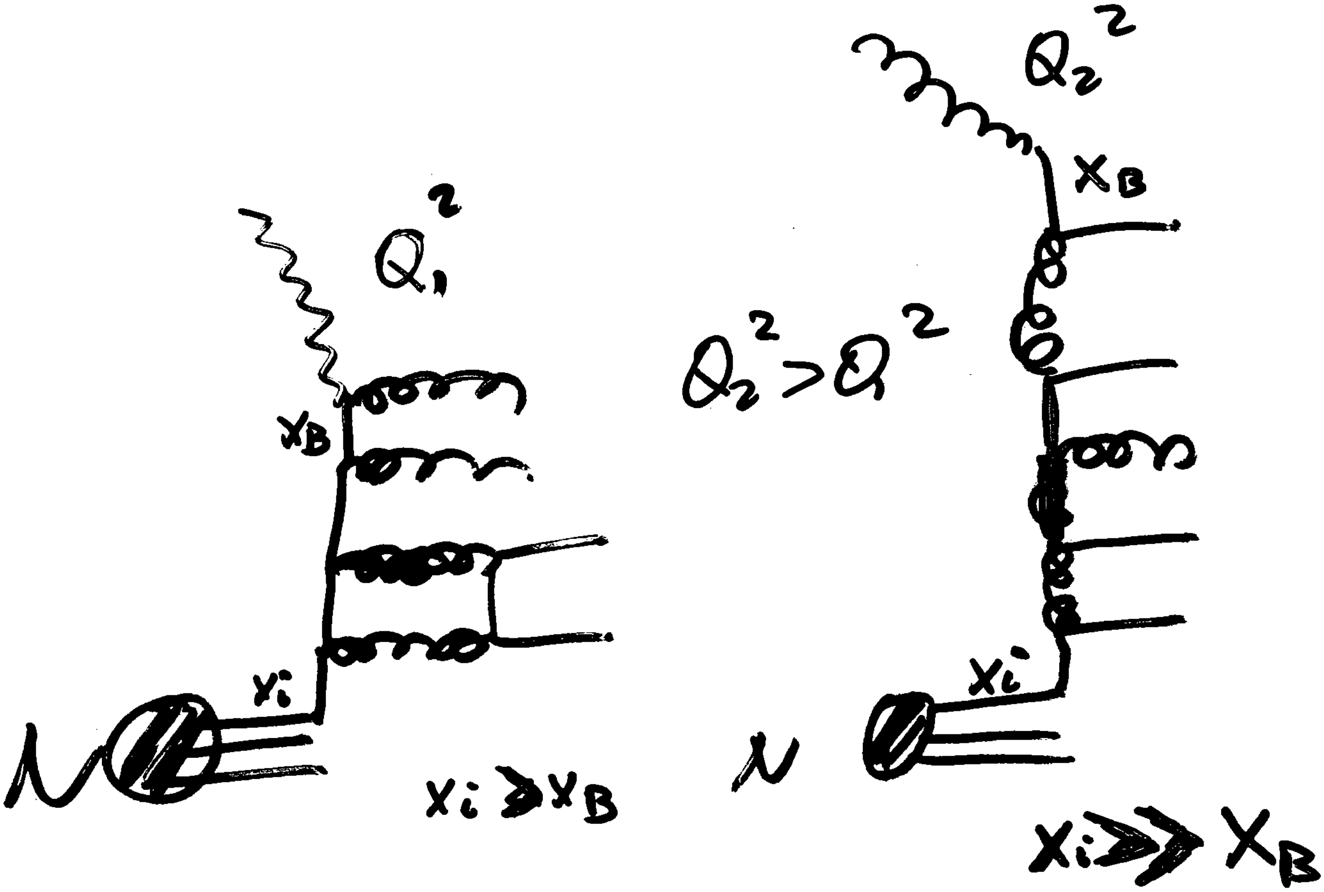

Small Q_0^2

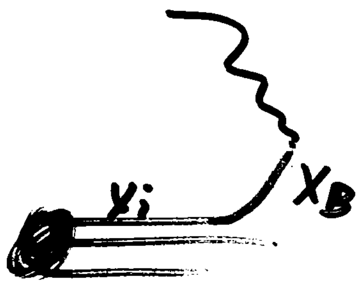

$x_i = x_B$

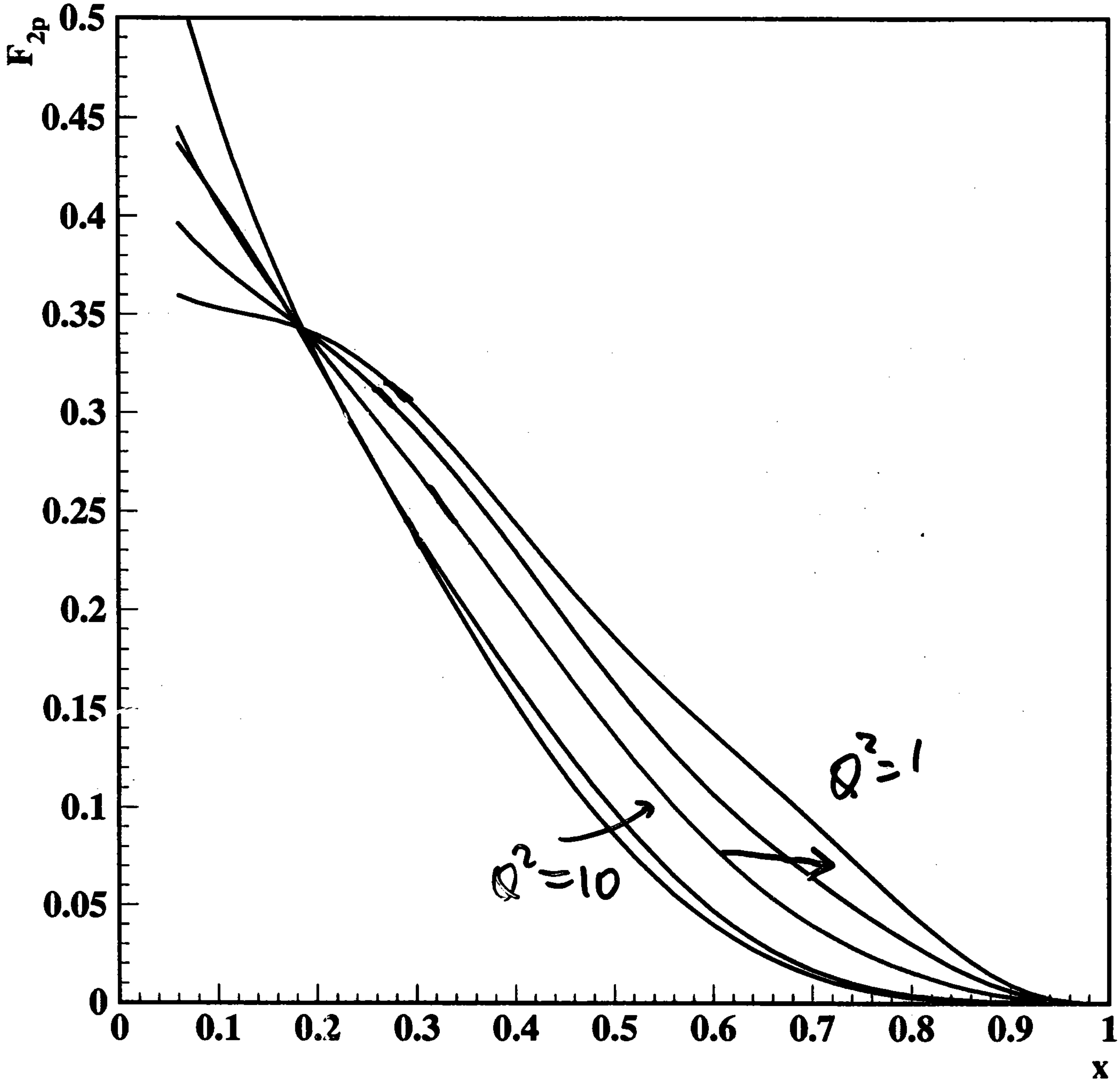

F2p
0.5
0.45
0.4
0.35
0.3
0.25
0.2
0.15
0.1
0.05
0
0
0.1
0.2
0.3
0.4
0.5
0.6
0.7
0.8
0.9
1
x
Q^2=1
Q^2=10

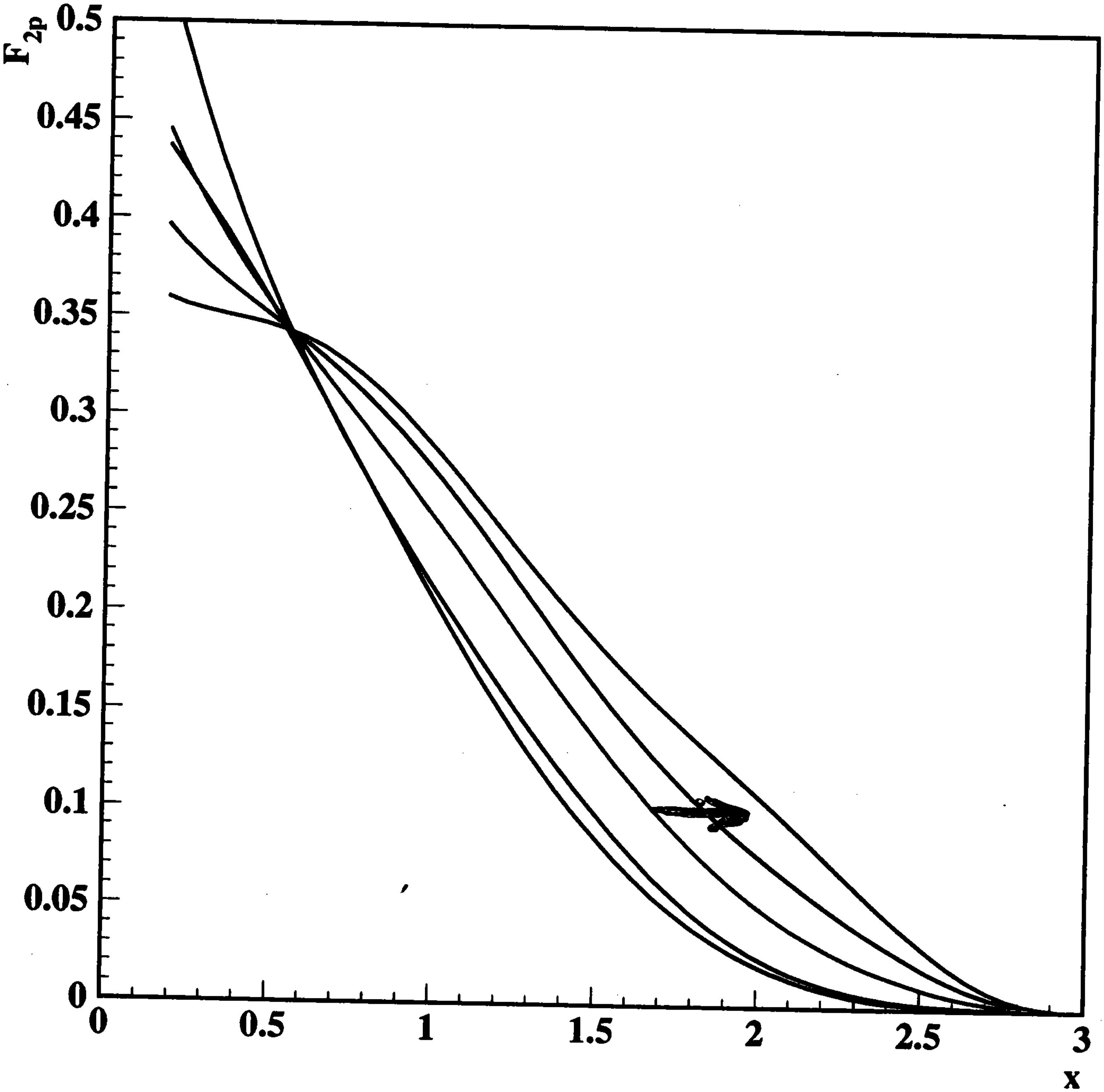

F2p
0.5
0.45
0.4
0.35
0.3
0.25
0.2
0.15
0.1
0.05
0
0
0.5
1
1.5
2
2.5
3
x

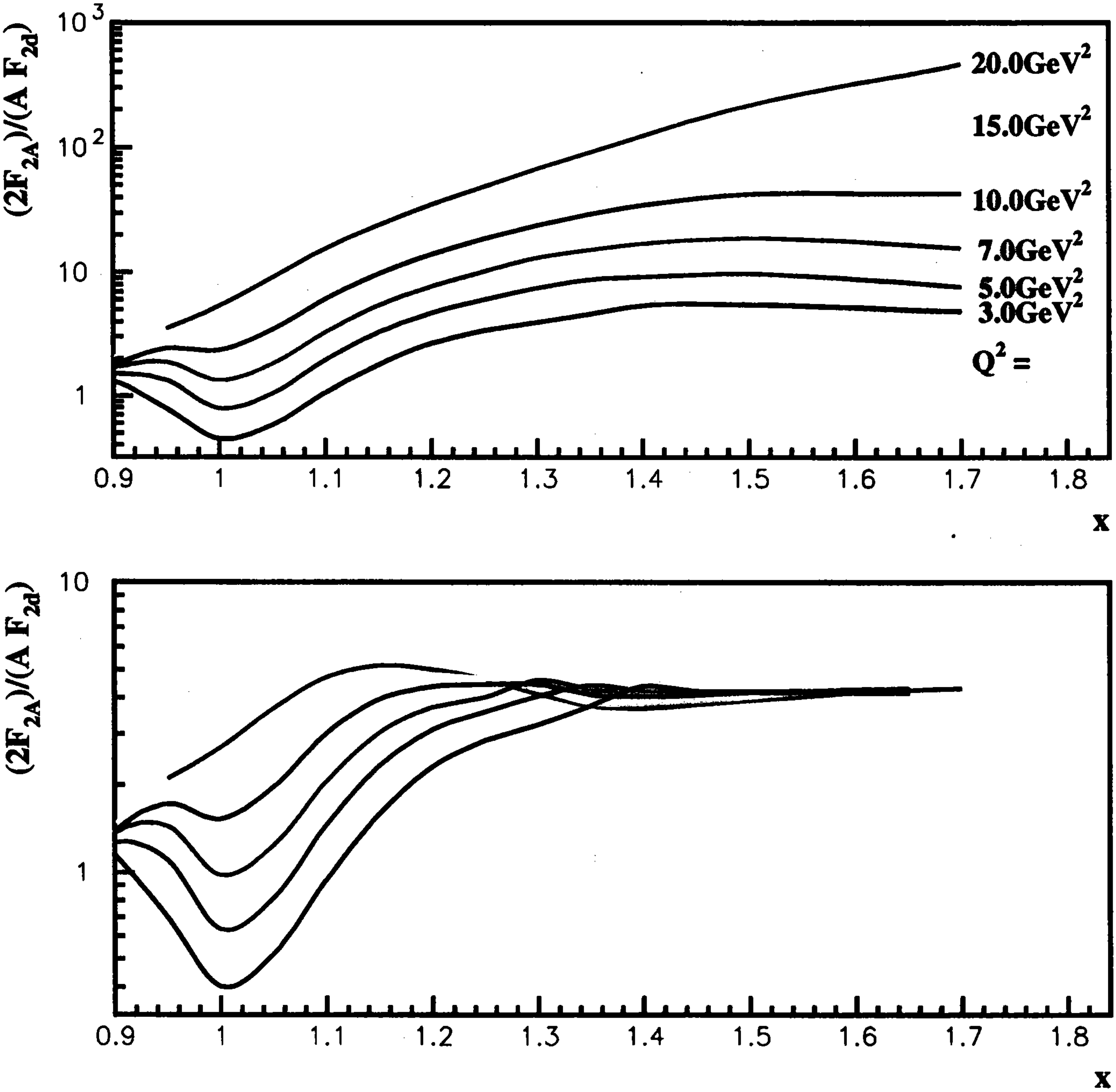

$(2F_{2A})/(A\ F_{2d})$
20.0GeV^2
15.0GeV^2
10.0GeV^2
7.0GeV^2
5.0GeV^2
3.0GeV^2
$Q^2 =$
x
$(2F_{2A})/(A\ F_{2d})$
x

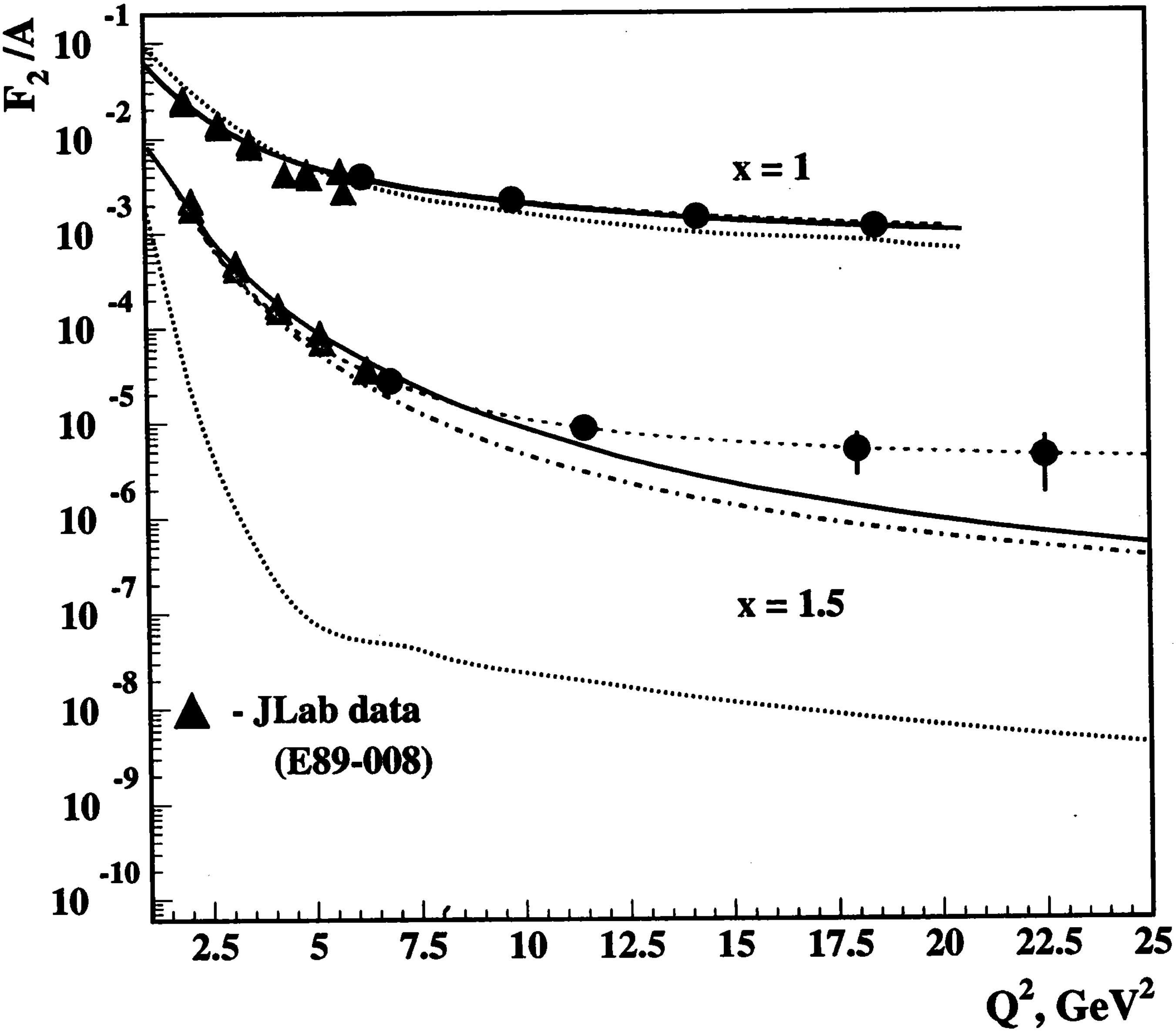

F2 /A
10 -1
10 -2
10 -3
10 -4
10 -5
10 -6
10 -7
10 -8
10 -9
10 -10
x = 1
x = 1.5
- JLab data
(E89-008)
2.5
5
7.5
10
12.5
15
17.5
20
22.5
25
Q2, GeV2

4L

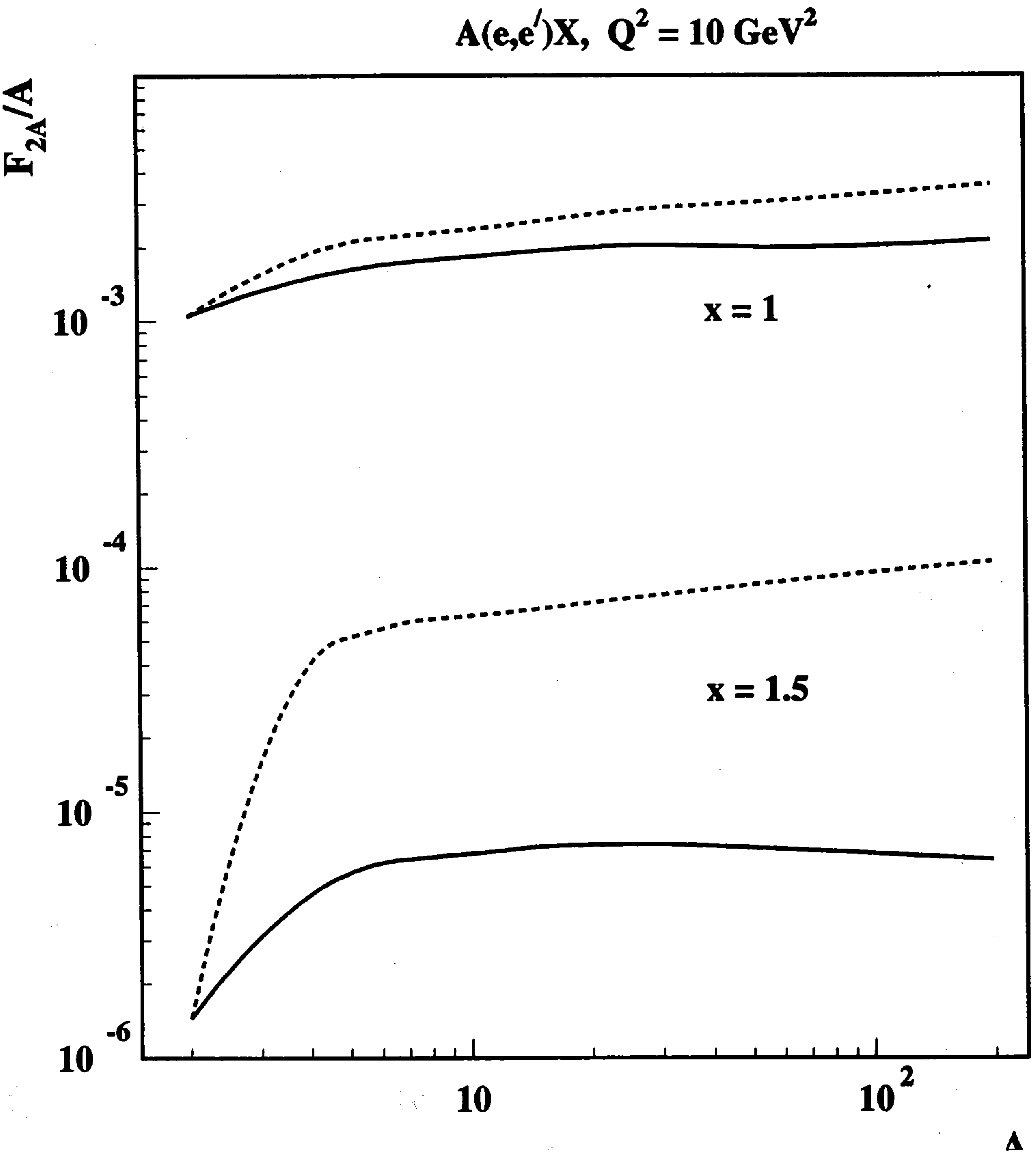

A(e,e′)X, Q² = 10 GeV²
F2A/A
10 -3
10 -4
10 -5
10 -6
x = 1
x = 1.5
10
10 2
A

$h_1 + h_2 \to h_3 + h_4$

$s, -t, -u \gg m^2, \quad \frac{t}{s} \ \frac{u}{s}$ FIXED

V. Probing the Strong Forces

- AGS is "closed"

- Confusion Theorem

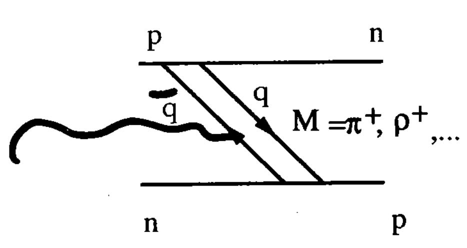

$\neq$

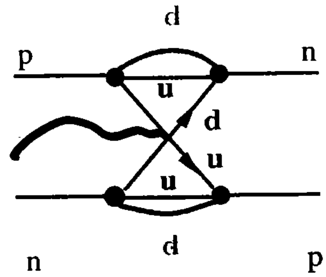

Meson Exchange ***Quark interchange***

MINIMAL FOCK COMPONENT OF THE NUCLEON

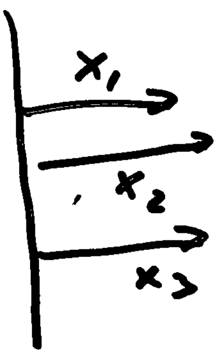

$x_1 + x_2 + x_3 = 1$

FEYNMAN PICTURE OF NUCLEON

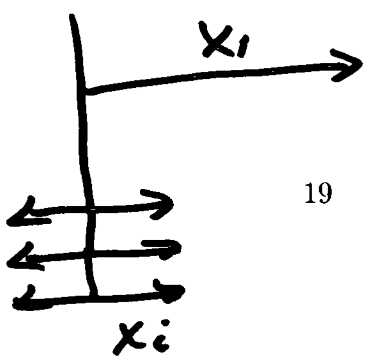

$x_1 \to 1$

$x_i \sim 0$

3.8. Beyond the NN Interaction

Identifying the basic origin of the NN force in the "nuclear physics approximation" is one of the fundamental tasks confronting us in our struggle to understand the role of QCD in making the world the way it is.

If we had only the forces in the NN system to guide us, this task would be made much more difficult. The reason is that there is a "confusion theorem" between the two leading contenders for the source of interhadronic potentials: meson exchange and quark exchange. The "theorem" is simple to understand: $q\bar{q}$ exchange leads to exactly the same t-channel quantum numbers as the exchange of a quark and "quark hole". Thus, while physically distinct (when two nucleons exchange a meson, at some intermediate time there are in addition to the original six quarks the extra $q\bar{q}$ pair; when two nucleons exchange quarks between themselves, there are never more than six quarks present), both mechanisms will lead one to an indentical parameterization of the effective NN potential. Without a quantitative understanding of how to calculate the strength of a given t-channel contribution, such parameterizations cannot disentangle the two mechanisms.

For this reason, studies of other interhadronic forces will probably be essential in unravelling the true origin of the NN force. The ΛN and ΣN systems are good places to start extending our knowledge of such forces and CEBAF at Jefferson Lab and FINUDA at DAPHNE have important roles to play. I believe it will also be vital to reach some understanding of the nature of the forces in other baryon-baryon channels like ΔN and $\Delta\Delta$, and also in mesonic channels. In this latter area, once again both CEBAF and KLOE at DAPHNE expect to make major contributions to our understanding of the $K\bar{K}$ system by defining the properties of the $f_0(980)$ and $a_0(980)$ as potential $K\bar{K}$ molecules (*i.e.*, mesonic analogues of the deuteron).

4. CONCLUSIONS

These examples of some key issues and experiments, which we will be part of writing into the history books how QCD leads to the phenomenon that make up the world around us, are necessarily superficial. However, I hope they will have provided a sense of the excitement that some of us feel as we begin this new era of strong interaction physics.

My optimism about the future is partly based on the existence of many new theoretical tools at hand: the large N_c expansion, the lattice, heavy quark expansions, and heavy baryon chiral perturbation theory.

However, it is especially significant for this field that new data is *at last* starting to appear. We are now seeing data from Bonn, Mainz, CLEO, SLAC, BNL, LEAR, and others. We will soon be seeing results from Hermes and a flood of new data from CEBAF at Jefferson Lab, RHIC at Brookhaven, and DAPHNE at Frascati Lab. In the longer term we can look forward to powerful new insights from the 50 GeV JHP project.

I conclude that there is every reason to believe that we are indeed on the threshold of a twenty year journey to complete our understanding of strongly interacting matter.

- Hard Exclusive Nuclear Reactions $\left\{ \begin{array}{c} s, -t \to \infty \\ -u \to \infty \\ \frac{t}{s}, \frac{u}{s} \text{ - fixed} \end{array} \right\}$

$$\gamma d \longrightarrow p n$$

90^c CM

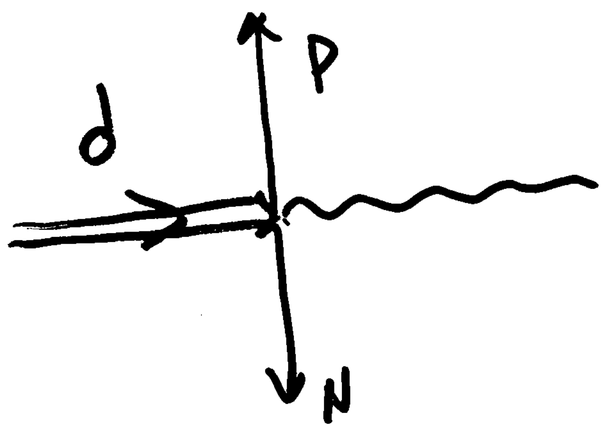

$P_{p,n} \sim 1\ GeV/c$

$E_\gamma = 2\ GeV$

$$\frac{d\sigma}{dt} \sim s^{-11} \sim s^{-(\overset{d}{6} + \overset{\gamma}{1} + \overset{p}{3} + \overset{n}{3} - 2)}$$

45

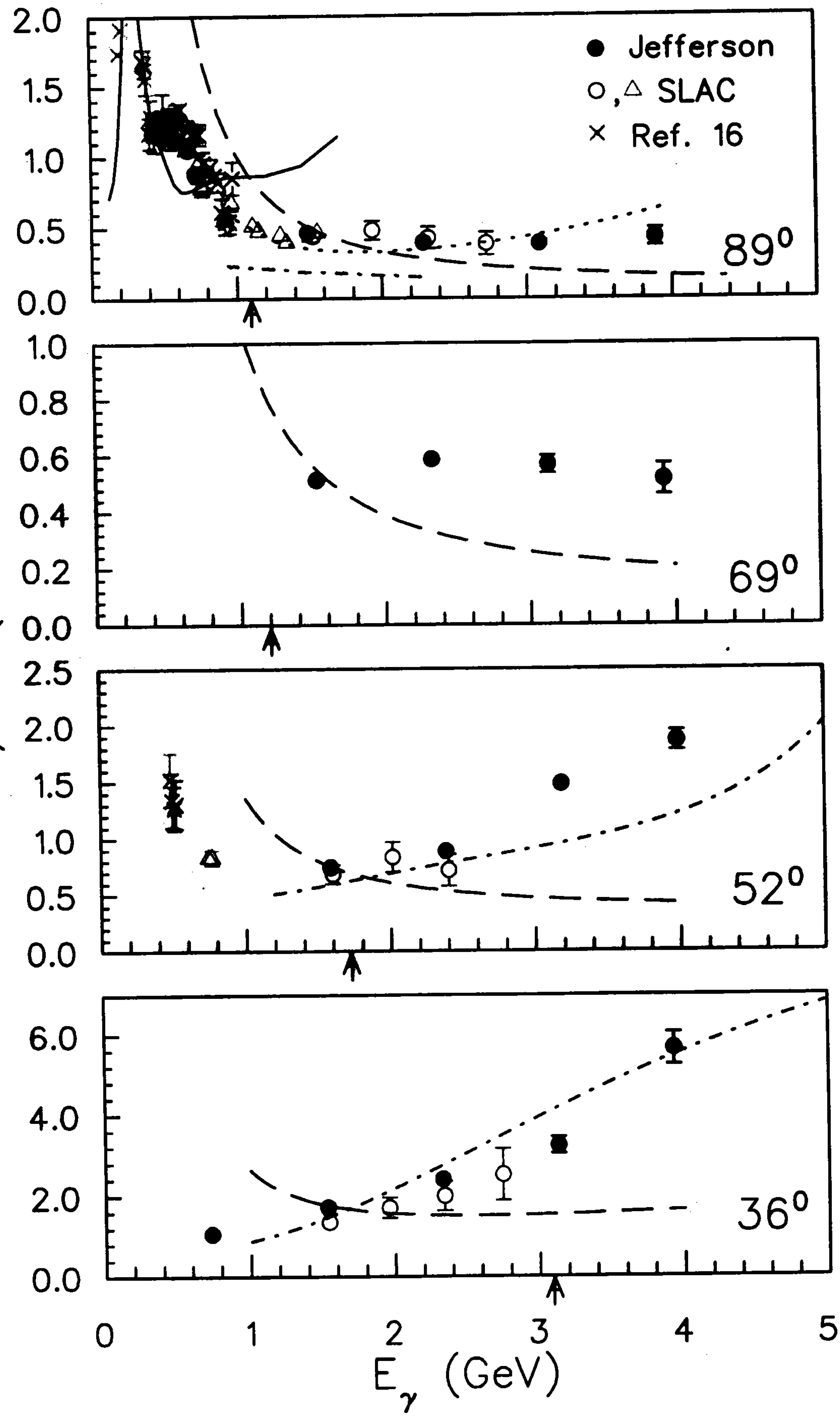

Jefferson
○, △ SLAC
× Ref. 16
89°
69°
52°
36°
$s^{11}d\sigma/dt$ (kb-GeV^{20})
E_γ (GeV)

${}^2D(\gamma p n)$

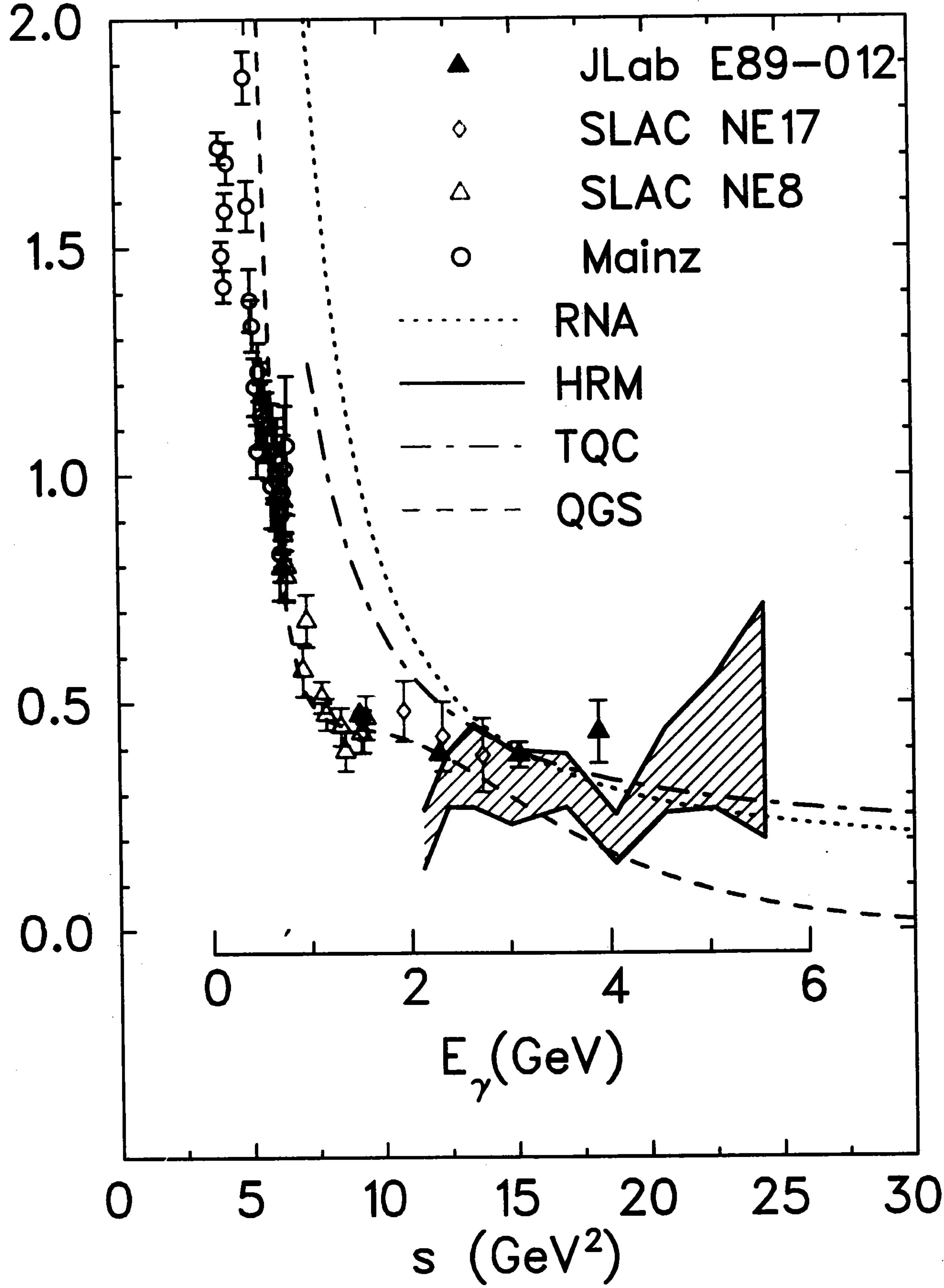

JLab E89–012
SLAC NE17
SLAC NE8
Mainz
RNA
HRM
TQC
QGS
$s^{11}d\sigma/dt$ (kb GeV^{20})
2.0
1.5
1.0
0.5
0.0
0
2
4
6
E_γ(GeV)
0
5
10
15
20
25
30
s (GeV^2)

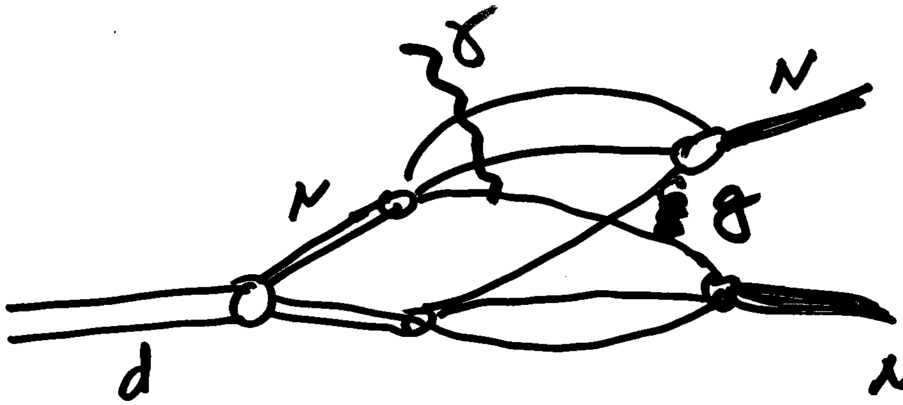

$$A = \psi_D \otimes A^{\gamma q} \otimes A^{np\to np}$$

exp

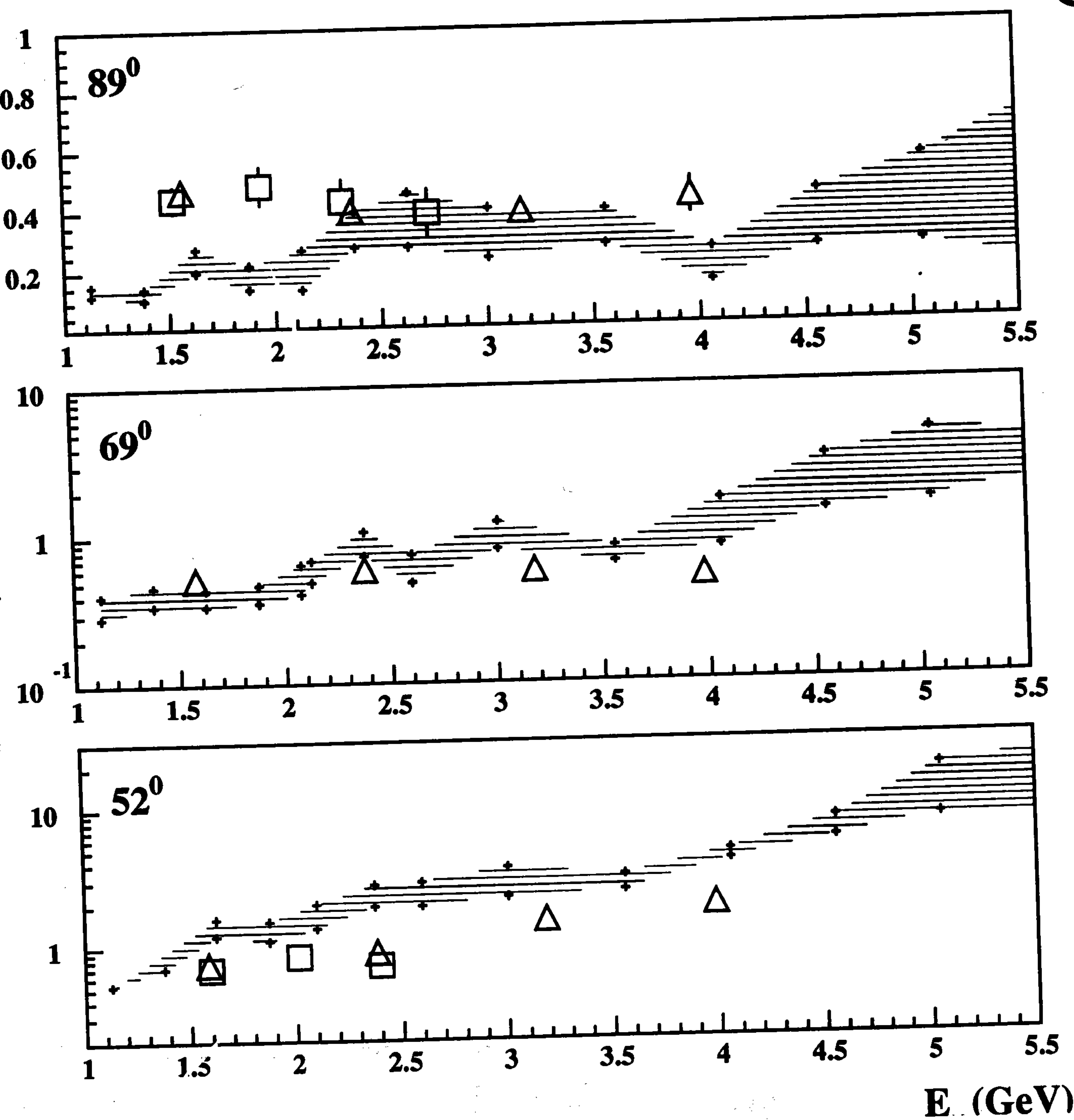

DISINTEGRATION OF THE PROTON PAIR

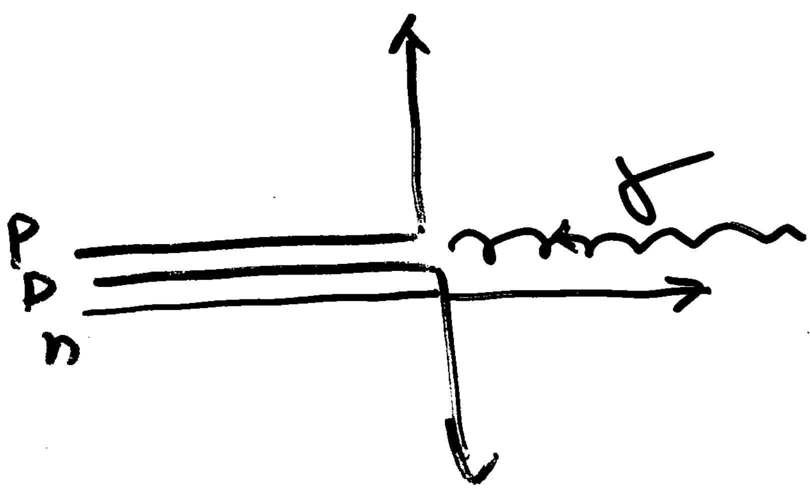

BRODSKY, FRANKFURT, GILMAN
HILLER, MILLER, PIASETZKY
SARGSIAN, STRIKMAN NUCL-TH-03

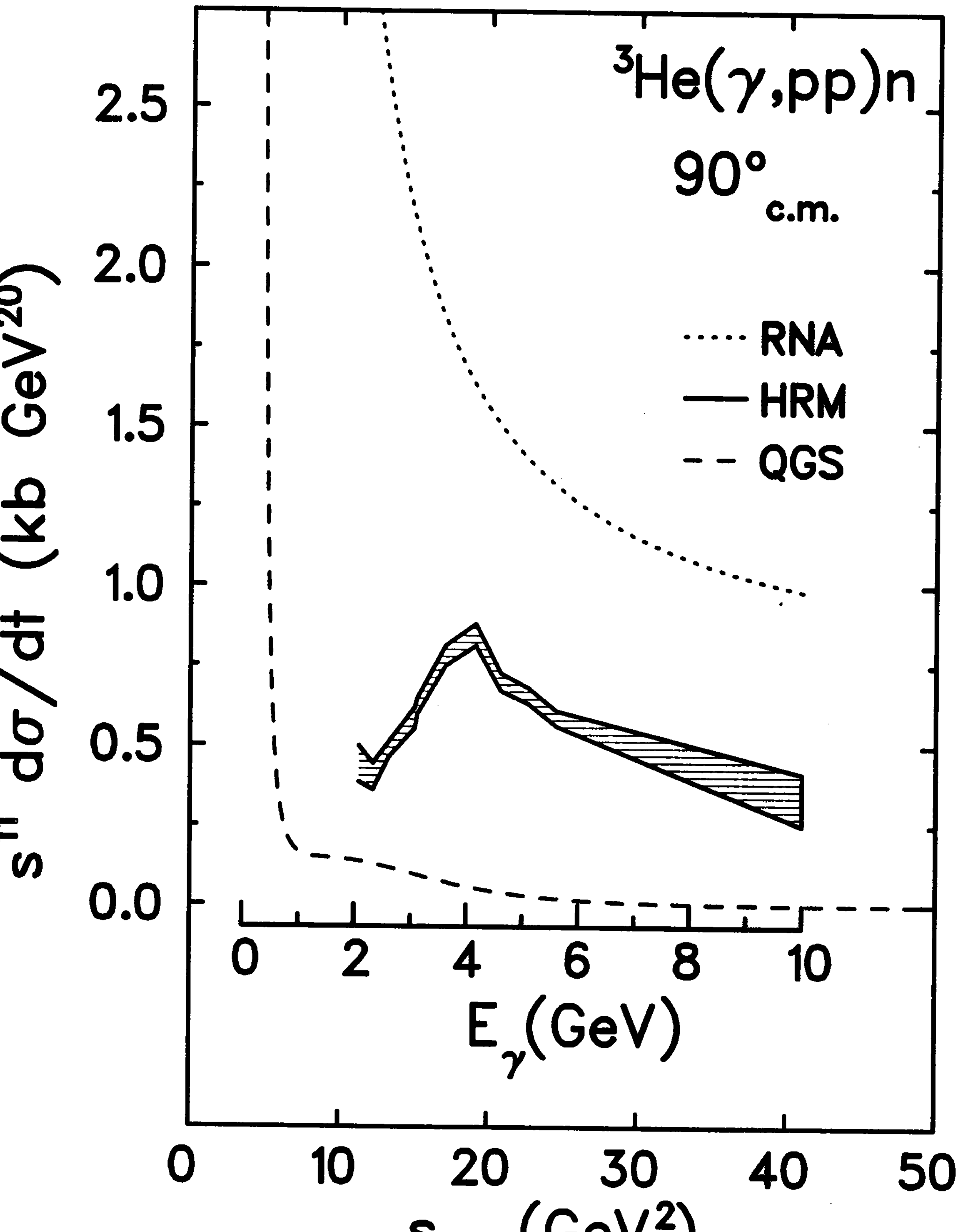

^{3}He(γ,pp)n
90°c.m.
RNA
HRM
QGS
2.5
2.0
1.5
1.0
0.5
0.0
s^{11} dσ/dt (kb GeV^{20})
0
2
4
6
8
10
E$_\gamma$(GeV)
0
10
20
30
40
50
s$_{pp}$ (GeV^2)

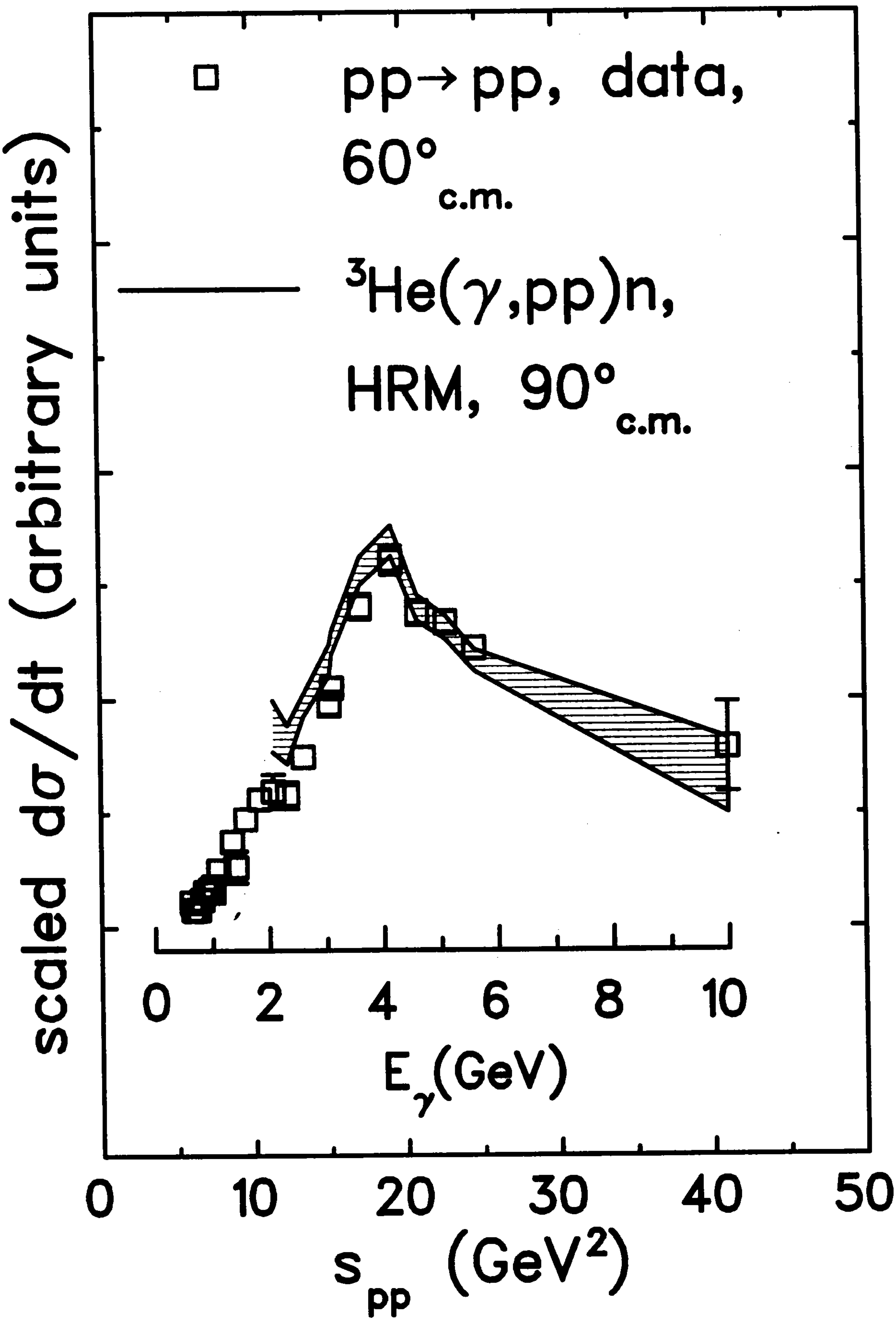

pp→pp, data,
60°c.m.
³He(γ,pp)n,
HRM, 90°c.m.
scaled dσ/dt (arbitrary units)
0
2
4
6
8
10
Eγ(GeV)
0
10
20
30
40
50
spp (GeV²)

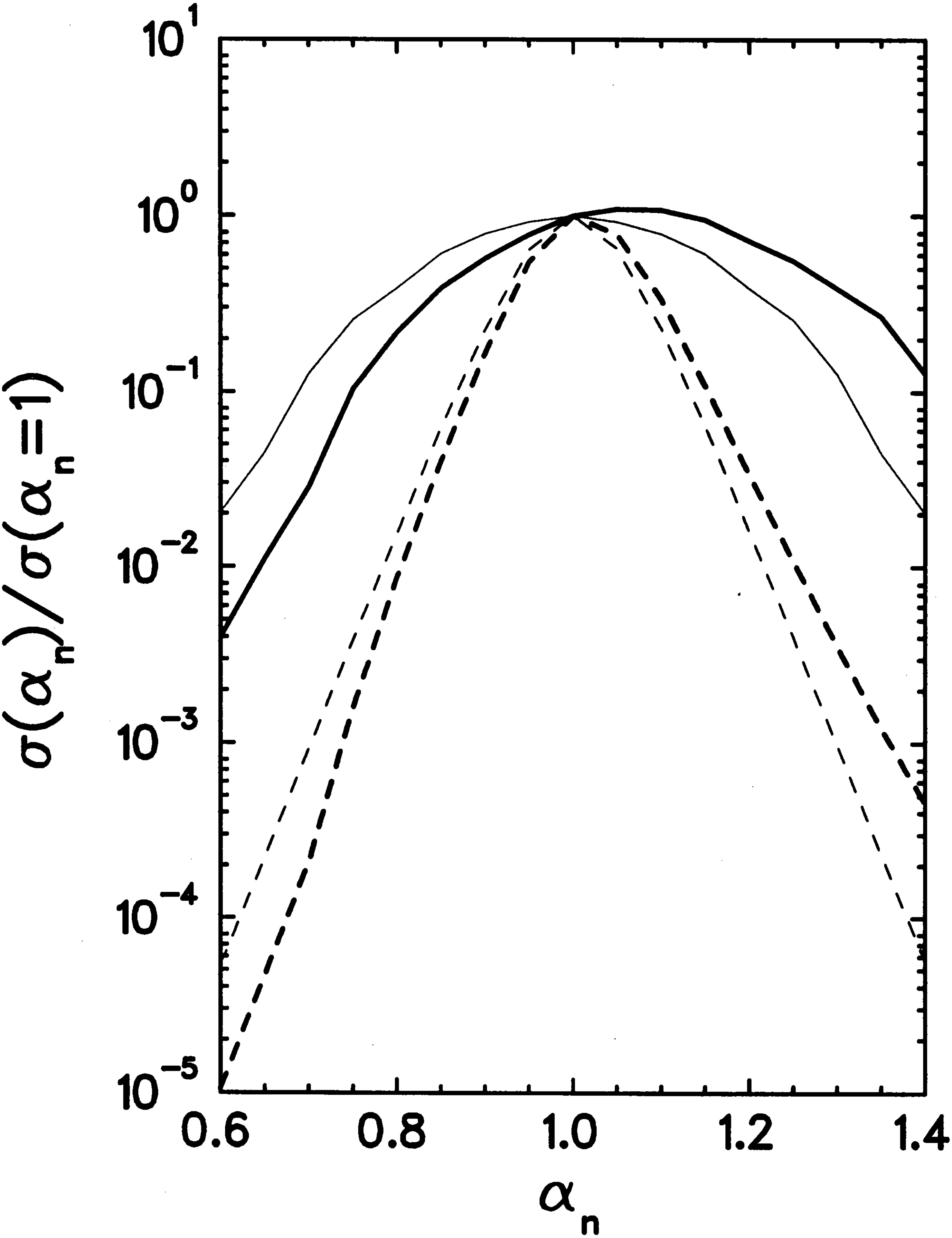

10^1
10^0
10^{-1}
10^{-2}
10^{-3}
10^{-4}
10^{-5}
0.6
0.8
1.0
1.2
1.4
α_n
$\sigma(\alpha_n)/\sigma(\alpha_n=1)$

$\gamma d \to \pi^- p \, p$

90° CM

IN GENERAL

$\gamma d \to h_1 B_1 B_2$

90^c CM

s - threshold

c - threshold

TABLE II. Measured transparencies for D, C, and Fe. The first uncertainty quoted is statistical, the second systematic. In the figures these are added in quadrature. The uncertainties in the figures do not include model-dependent systematic uncertainties on the simulations. We note that a renormalization of these nuclear transparencies with a factor of 1.020 (T_C) and 0.896 (T_{Fe}) is advocated in Ref. [30].

Q^2 $(\mathrm{GeV}/c)^2$	T_D	T_C	T_{Fe}
3.3	0.897±0.013±0.027	0.548±0.005±0.013	0.394±0.009±0.009
6.1	0.917±0.013±0.028	0.570±0.007±0.013	0.454±0.015±0.018
8.1	0.867±0.020±0.026	0.573±0.010±0.013	0.391±0.012±0.009

cision than of Refs. [8,9,27]. Our results at $Q^2 = 3.3$ $(\mathrm{GeV}/c)^2$ agree well with the previous results for deuterium [8,9], carbon, and iron [16].

Little or no Q^2 dependence can be seen in the nuclear transparency data above $Q^2 \approx 2$ $(\mathrm{GeV}/c)^2$. Excellent constant-value fits can be obtained for the various transparency results above such Q^2. For deuterium, carbon, and iron, fit values are obtained of 0.904 (±0.013) 0.570 (±0.008), and 0.403 (±0.008), with χ^2 per degree of freedom of 0.56, 1.29, and 1.17, respectively. As in Ref. [16], we compare with the results from correlated Glauber calculations, including rescattering through third order [28], depicted as the solid curves for $0.2<Q^2<8.5$ $(\mathrm{GeV}/c)^2$. In the case of deuterium, we show (dashed curve) a generalized Eikonal approximation calculation, coinciding with a Glauber approximation for small missing momenta [29]. The Q^2 dependence of the nuclear transparencies is well described, but the transparencies are underpredicted for the heavier nuclei. This behavior persists even taking into account the model-dependent systematic uncertainties.

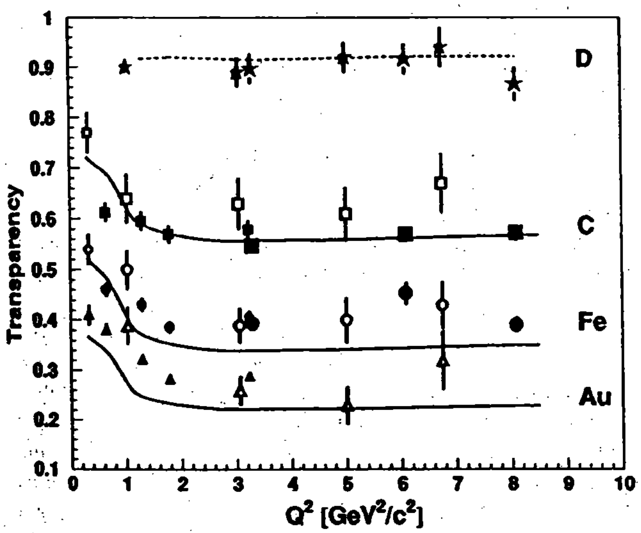

FIG. 4. Transparency for $(e,e'p)$ quasielastic scattering from D (stars), C (squares), Fe (circles), and Au (triangles). Data from the present work are the large solid stars, squares, and circles, respectively. Previous JLab data (small solid squares, circles, and triangles) are from Ref. [16]. Previous SLAC data (large open symbols) are from Refs. [8,9]. Previous Bates data (small open symbols) at the lowest Q^2 on C, Ni, and Ta targets, respectively, are from Ref. [27]. The errors shown for the current measurement and previous measurement [16] include statistical and the point-to-point systematic (±2.3%) uncertainties, but do not include model-dependent systematic uncertainties on the simulations or normalization-type errors. The net systematic errors, adding point-to-point, normalization-type and model-dependent errors in quadrature, are estimated to be (±3.8%), (±4.6%), and (±6.2%) corresponding to D, C, and Fe, respectively. The error bars for the other data sets [8,9,27] include their net systematic and statistical errors. The solid curves shown from $0.2<Q^2<8.5$ $(\mathrm{GeV}/c)^2$ are Glauber calculations from Ref. [28]. In the case of D, the dashed curve is a Glauber calculation from Ref. [29].

Recently, a new calculation of nuclear transparencies has become available [30]. This results in a better agreement between Glauber calculations and the A dependence of the nuclear transparency data. In this paper [30] it was argued that the uncertainty in the treatment of short-range correlations in the Glauber calculation can be constrained with inclusive $A(e,e')$ data. This results in an effective renormalization of the nuclear transparencies for the ^{12}C and ^{56}Fe nucleus of 1.020 and 0.896, respectively. Such a renormalization is due to integration of the denominator in Eq. (2) over a four-dimensional phase space V in E_m and $|\vec{p}_m|$ argued to be more consistent with experiments. That is, the experiment measures an angular distribution in the scattering plane rather than the complete $|\vec{p}_m|<300$ MeV/c region. This reduces the influence of short-range correlations. The nuclear transparencies as given in Table II would have to be multiplied by these renormalization factors, rendering value more consistent with the A dependence of Glauber calcula tions. Although such a renormalization may be appropriate we quote nuclear transparency numbers consistent with th procedure of Refs. [8,9,16], for the sake of comparison.

For the remainder of this section, we will concentrate on a combined analysis of the world's $A(e,e'p)$ nuclear transpar ency data. Figure 5 shows T as a function of A. The curve represent empirical fits of the form $T=cA^{\alpha(Q^2)}$, using th deuterium, carbon, and iron data. We find, within uncertain ties, the constant c to be consistent with unity as expecte and the constant α to exhibit no Q^2 dependence up to Q $=8.1$ $(\mathrm{GeV}/c)^2$. A similar treatment to nuclear transparenc results of the older $A(e,e'p)$ experiments renders a nearl constant value of $\alpha=-0.24$ for $Q^2 \geq 1.8$ $(\mathrm{GeV}/c)^2$. Nu merical values are presented in Table III. We note that usin the renormalizations of the nuclear transparencies propose by Frankfurt, Strikman, and Zhalov [30] would reduce th

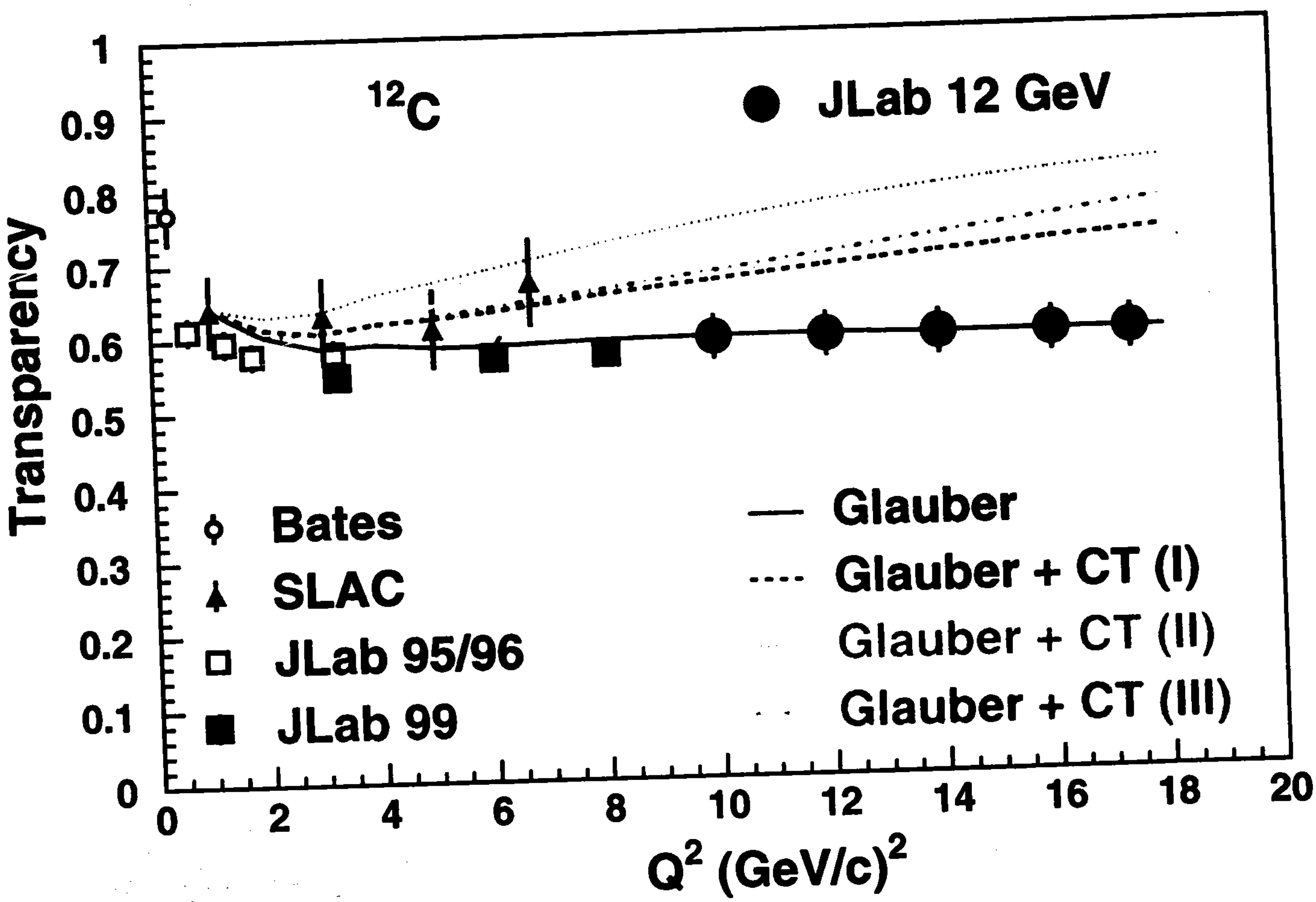

12C
JLab 12 GeV
Transparency
Q2 (GeV/c)2
Bates
SLAC
JLab 95/96
JLab 99
Glauber
Glauber + CT (I)
Glauber + CT (II)
Glauber + CT (III)

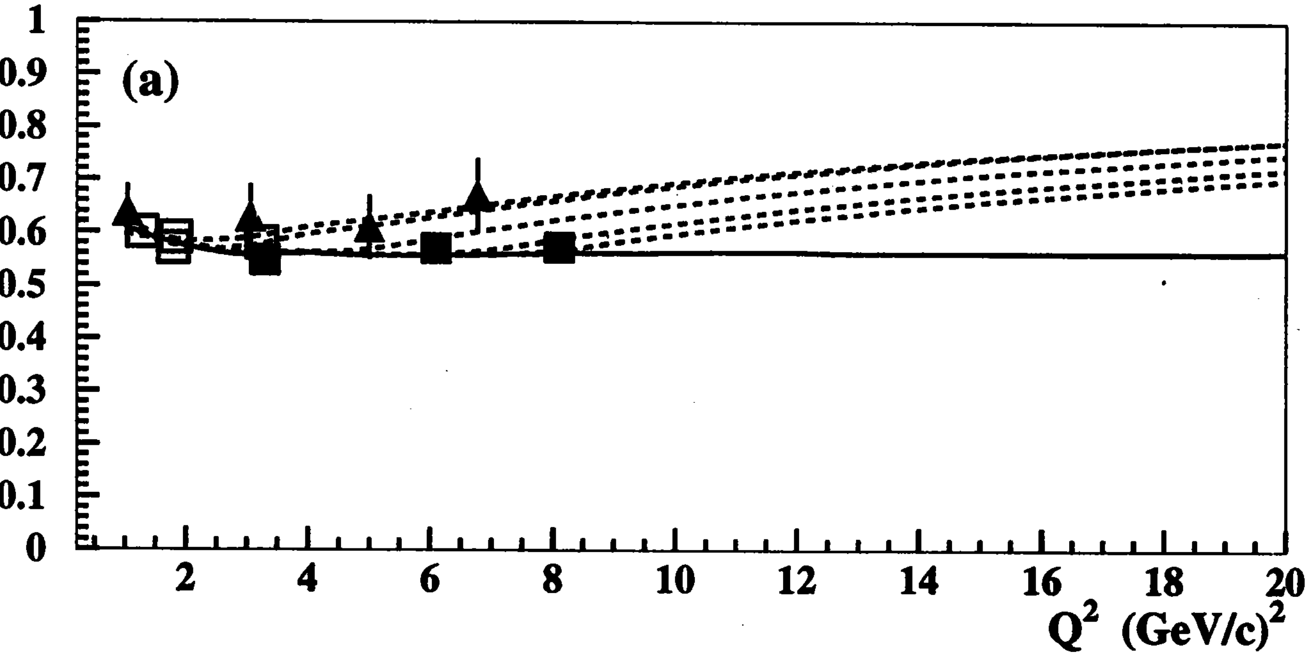

(a)
1
0.9
0.8
0.7
0.6
0.5
0.4
0.3
0.2
0.1
0
2
4
6
8
10
12
14
16
18
20
Q^2 (GeV/c)^2

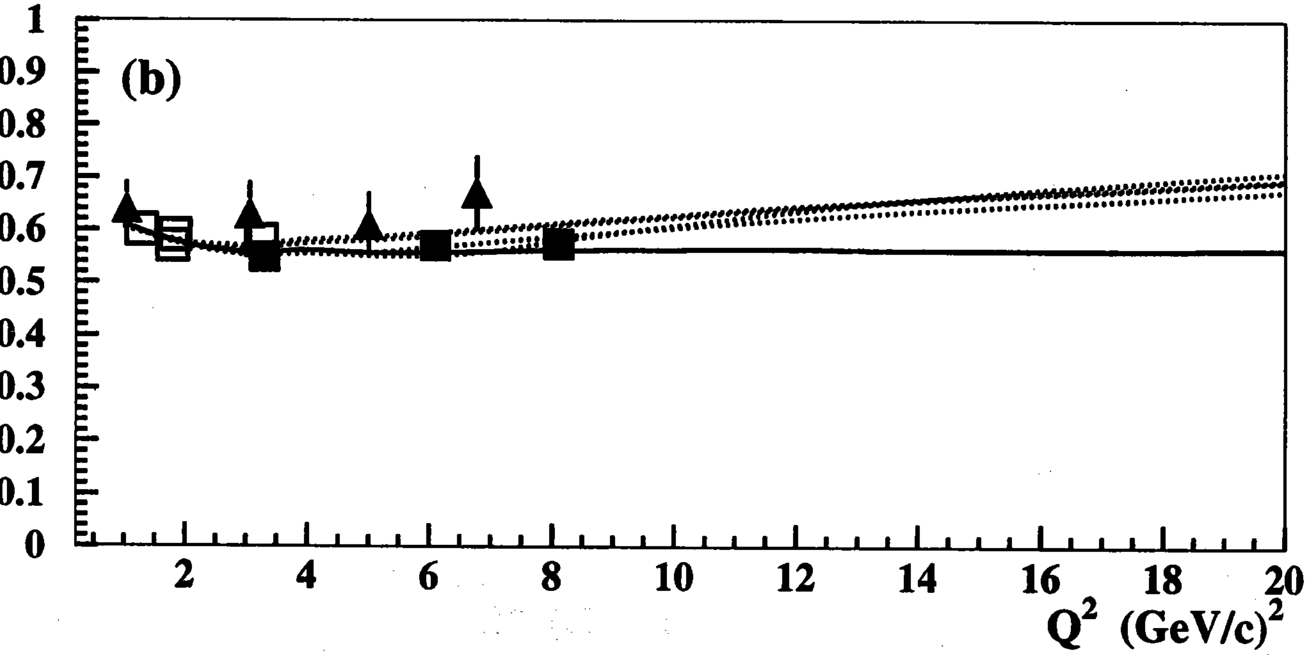

(b)
1
0.9
0.8
0.7
0.6
0.5
0.4
0.3
0.2
0.1
0
2
4
6
8
10
12
14
16
18
20
Q^2 (GeV/c)^2

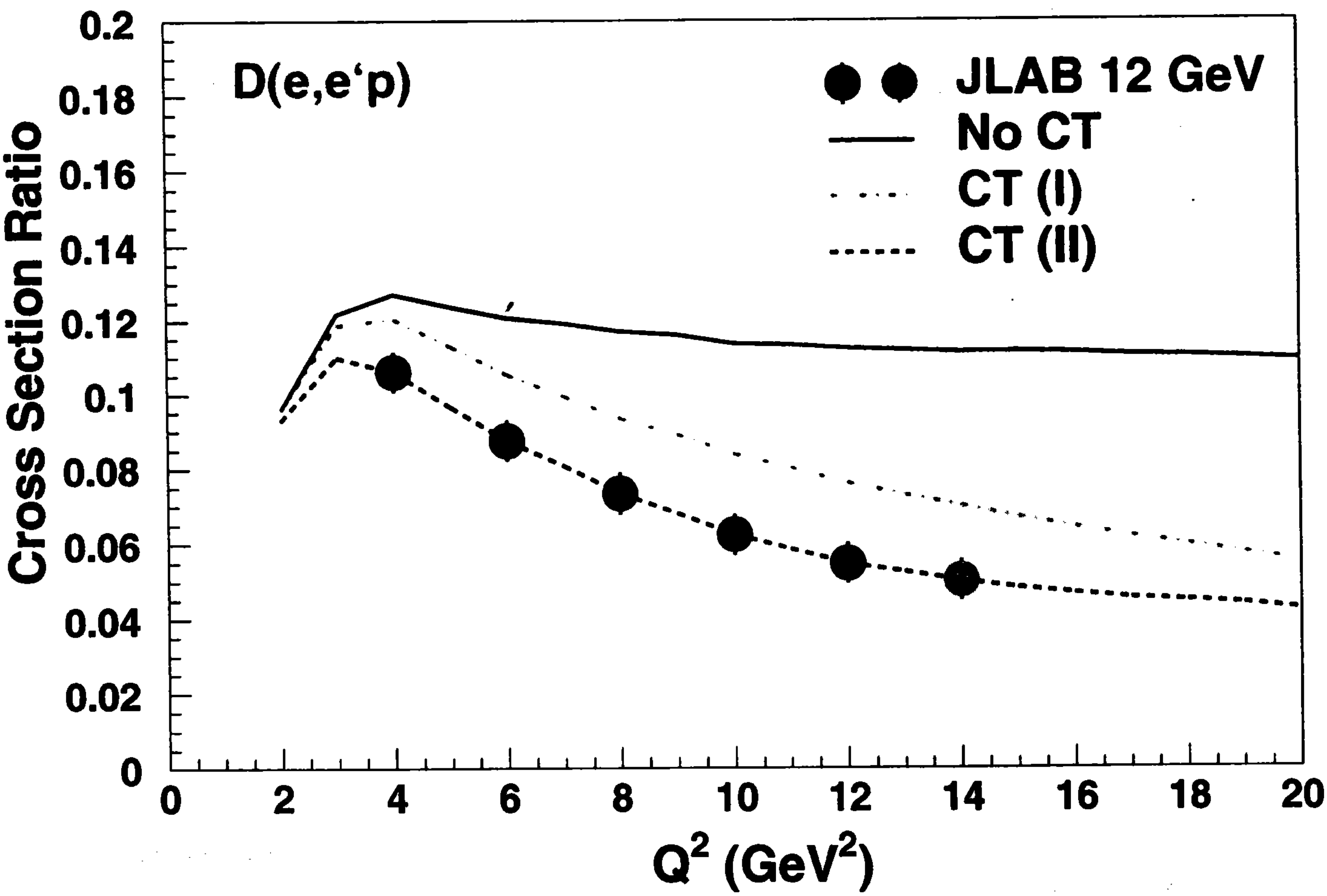

D(e,e'p)
JLAB 12 GeV
No CT
CT (I)
CT (II)
Cross Section Ratio
0.2
0.18
0.16
0.14
0.12
0.1
0.08
0.06
0.04
0.02
0
0
2
4
6
8
10
12
14
16
18
20
Q^2 (GeV^2)

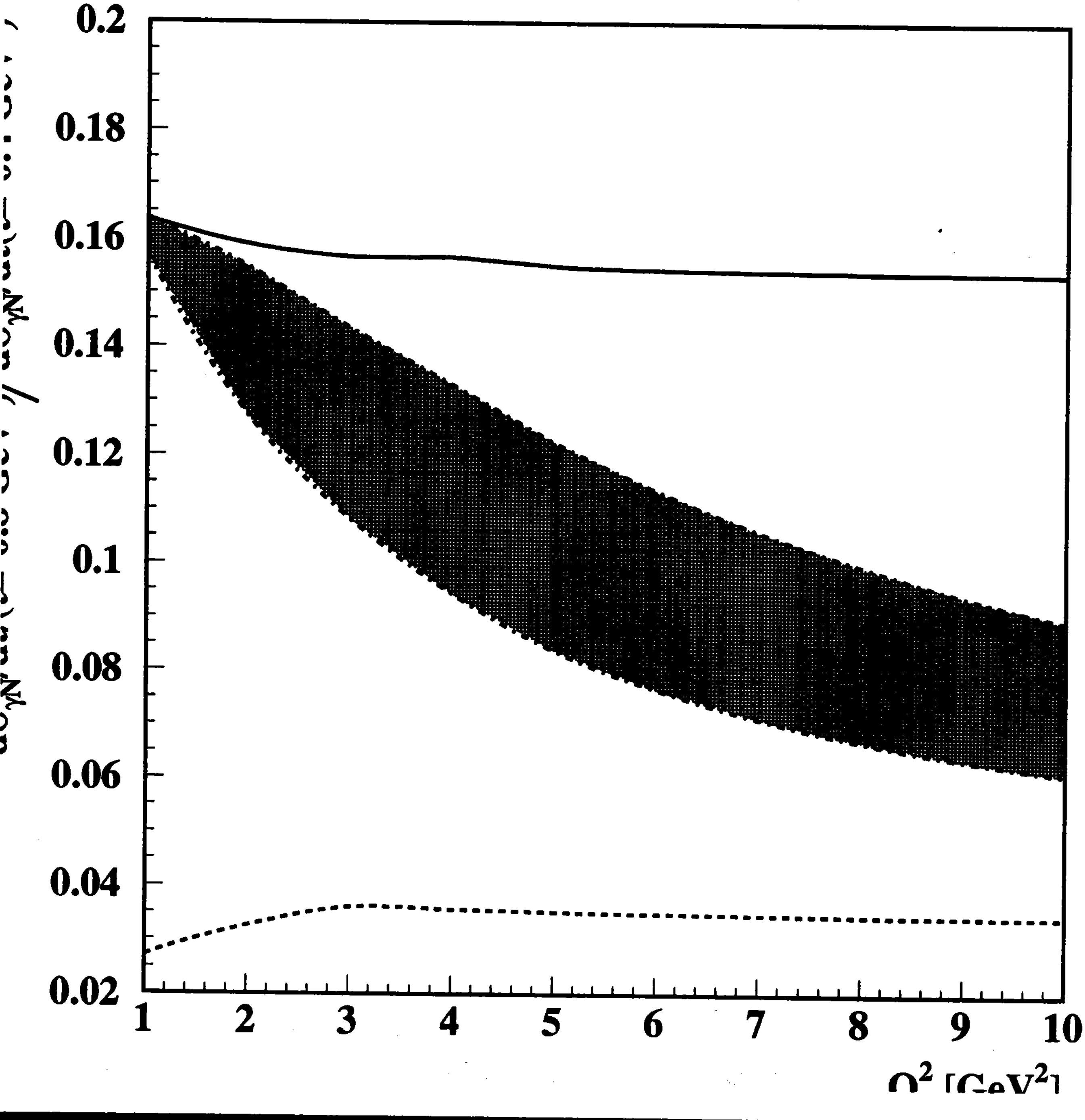
0.2
0.18
0.16
0.14
0.12
0.1
0.08
0.06
0.04
0.02
1
2
3
4
5
6
7
8
9
10

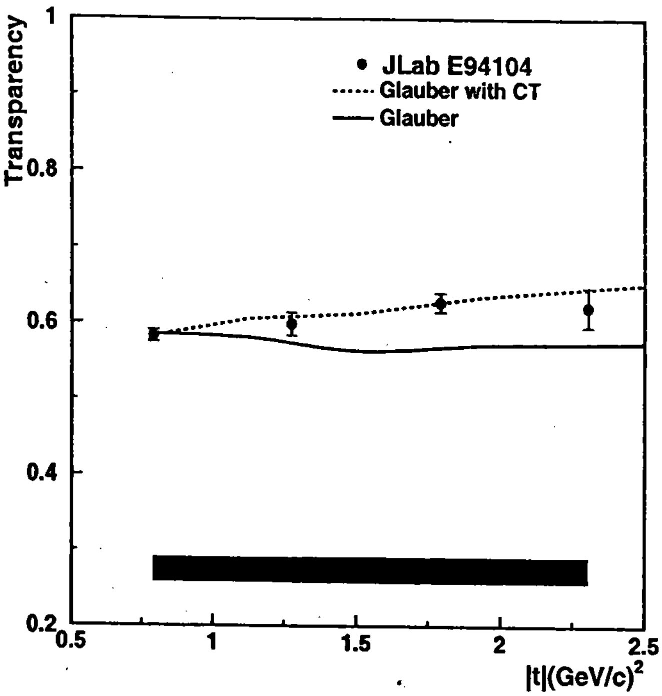

FIG. 2: The nuclear transparency of ^{4}He(γ,p π^-) at 70° C. M. angle, as a function of momentum transfer square $|t|$. The error bars shown are statistical uncertainties only. The dark band shows the point-to-point systematic uncertainty. The total systematic uncertainty is 4.8%.

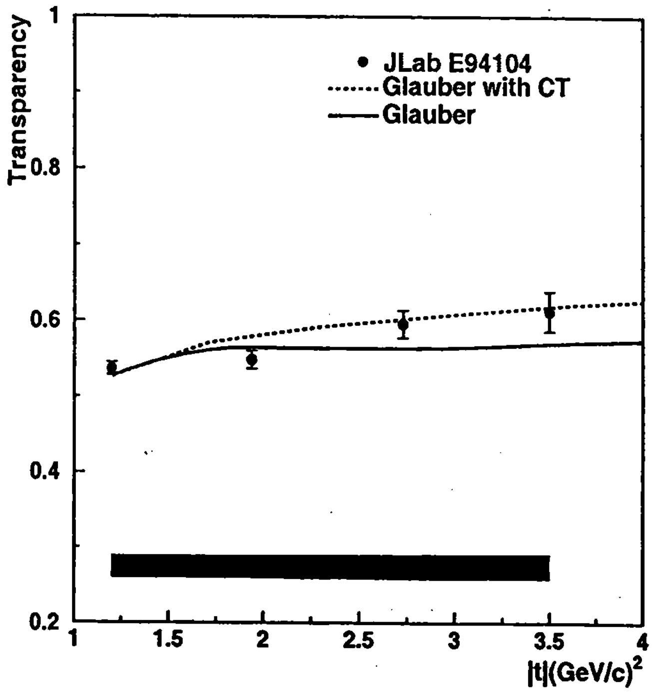

FIG. 3: The nuclear transparency of ^{4}He(γ,p π^-) at 90° C. M. angle, as a function of momentum transfer square $|t|$. The error bars shown are statistical uncertainties only. The dark band shows the point-to-point systematic uncertainty. The total systematic uncertainty is 4.8%.

tion appears to deviate from the data at the higher energies. The absolute magnitude of the calculations with CT seem to disagree with the measurement, however, it is the momentum transfer squared ($|t|$) dependence of the transparency which is of greater significance. The $|t|$ dependence is not affected by the normalization systematic uncertainties. The slopes of the measured transparency obtained from the three points which are above the resonance region (above E_γ = 2.25 GeV) are shown in Table II. These slopes are consistent, within experimental uncertainties, with the slopes predicted by the calculations with CT and they disagree with the Glauber calculations at the $\approx 1\ \sigma$ ($2\ \sigma$) level for θ_{cm} = 70° (90°). It is also interesting that the results are consistent with the rise expected for CT at the same photon energy at which the onset of scaling behavior was observed in the cross-section for the γ n $\rightarrow$ π^- p and the γ p $\rightarrow$ π^+ n processes [19]. Thus, these data suggest the onset of CT-like behavior, but future experiments with significantly improved statistical and systematic precision are essential to put this result on a firmer statistical basis.

In conclusion we have measured the nuclear transparency for the fundamental process γ n $\rightarrow$ π^- p on the ^{4}He target at θ_{cm} = 70° and 90° in the photon energy range from 1.1 to 4.5 GeV. These measurements establish the baseline for the study of nuclear transparency in photo-pion reactions and provide important tests of calculations based on the standard model of nuclear physics and on Glauber theory. The measured transparency shows a very interesting momentum transfer squared dependence which deviates from the standard nuclear physics predictions at the higher momentum transfers. The observed momentum transfer squared dependence of the nuclear transparency is consistent with that predicted for the color transparency effect. Future experiments with better statistical and systematic precision in this energy range together with improved theoretical calculations are crucial for confirming these results.

TABLE II: The slope for the $|t|$ dependence of the extracted nuclear transparency obtained from the three points which are above the resonance region (above $\sqrt{s}$ = 2.25 GeV). The uncertainties are statistical and systematic respectively.

C.M. angle	Measured slope	CT	Glauber
(deg)	(GeV/c)$^{-2}$	(GeV/c)$^{-2}$	(GeV/c)$^{-2}$
70	0.032 ± 0.027 ± 0.022	0.037	0.009
90	0.046 ± 0.016 ± 0.014	0.024	0.006

We acknowledge the outstanding support of JLab Hall A technical staff and Accelerator Division in accomplish-

I believe we will eventually appreciate that only Yukawa's original meson will survive as a distinct contributor to interhadronic forces, while other mesons and quark exchange will be merged into a single comprehensive nuclear theory of the future

Nathan Isgur, "The Quark Structure of Matter, JLAB-THY-97-15